STRUCTURAL, GEOCHEMICAL AND ISOTOPIC INVESTIGATION OF GRANITOIDS WITHIN THE CENTRAL AREA OF THE EASTERN WEEKEROO INLIER, OLARY DOMAIN, SOUTH AUSTRALIA.

Damian Brett (B. Sc.)

Department of Geology and Geophysics
University of Adelaide

This thesis is submitted as a partial fulfilment for the
Honours Degree of Bachelor of Science

November 1998

National Grid Reference
(SI 54-2) 1:250 000

ABSTRACT

In the central part of the eastern Weekeroo Inlier, Olary Domain, two types of granite have been identified. This thesis explores both granite types in order to explain possible tectonic environments and geological evolution during the Proterozoic.

The A-type Walter Outalpa granite is characterised by high SiO_2, Zr, Nb, Y, rare earth elements (REE) and low MgO, CaO, TiO_2, P_2O_5 and light field strength elements (LFSE). High zircon saturation temperatures differentiate this fractionated A-type granite from potential fractionated I-type granites. The peraluminous granite is characterised by high SiO_2, Al_2O_3, Rb, U, Th, and low MgO, CaO, TiO2, Sr and light REE. It displays strong geochemical similarities to the Bimbowrie S-type granite.

Consistent geochemical and isotopic characteristics for the Walter Outalpa granite and other similar A-type granites across the Olary Domain indicate a single regional crustal plus mantle source. Partial melting of lower Archaean crust due to lithospheric thinning is proposed. Geochemistry and isotopic analysis of the peraluminous granites suggest varying infracrustal sources for loosely grouped S-type granites in the Olary Domain.

Previous interpretations for the depositional environment of the Willyama Supergroup metasediments in a continental rift setting are supported by comagmatic A-type volcanics and granites within the central part of the eastern Weekeroo Inlier. An extensional environment during emplacement is consistent with evidence for shallow level emplacement such as graphic texture, and the absence of a contact aureole for the Walter Outalpa granite.

There is foliation development and evidence of folding for three deformation events during the Proterozoic Olarian Orogeny. Timing relationships between granitoids and metasediments in this area have constrained relative timing of emplacement. Low temperature solid state deformation affected the A-type Walter Outalpa granite after emplacement into Willyama Supergroup metasediments. Crosscutting relationships between the peraluminous granite and adjacent deformed metasediments imply a late to post D_2 emplacement for this granite.

TABLE OF CONTENTS

CHAPTER 1

INTRODUCTION

1.1 Review of literature 1

1.1.1 Problem of timing of granitic emplacement in gneissic terrain 1

1.1.2 Correlating and classifying granitoids 1

1.2 Aims and methods 2

CHAPTER 2

REGIONAL GEOLOGY

2.1 Geological setting 3

2.2 Stratigraphy 3

2.3 Igneous activity 5

2.4 Deformation 6

2.5 Metamorphism 8

CHAPTER 3

LITHOLOGICAL VARIATION WITHIN THE GNEISS COMPLEX OF THE CENTRAL EASTERN WEEKEROO INLIER

3.1 Metasediments 9

3.1.1 Layered gneiss 9

3.1.2 Migmatite 10

3.1.3 Andalusite schist 10

3.1.4 Calcsilicate 10

3.1.5 Albitite (meta-rhyolite) 10

3.1.6 Sheared gneiss 11

3.1.7 Quartz augen gneiss 11

3.2 Intrusives 11

3.2.1 Walter Outalpa granite 11

3.2.2 Peraluminous granite 12

3.2.3 Pegmatite 13

3.2.4 Amphibolite 13

3.3 Magnetics of the central eastern Weekeroo Inlier 13

CHAPTER 4

STRUCTURAL DESCRIPTION OF GNEISS COMPLEX, CENTRAL EASTERN WEEKEROO INLIER

4.1 Foliations 14

4.1.1 S_0/S_1 in metasediments 14

4.1.2 S_2 in metasediments 14

4.1.3 S_3 in metasediments 15

4.1.4 Foliation in the Walter Outalpa granite 15

4.1.5 Foliation in the peraluminous granite 16

4.2 Folding 16

4.2.1 First generation folds (F_1) 16

4.2.2 Second generation folds (F_2) 16

4.3 Faulting and Shearing 17

4.4 Metamorphism 17

4.5 Metasediment – Granitoid Relationship 17

4.6 Discussion on the timing of the Walter Outalpa granite 19

CHAPTER 5

GEOCHEMICAL INVESTIGATION

5.1 Geochemical signature of intrusives 20

5.1.1 Walter Outalpa granite 20

5.1.2 Mafic enclaves 21

5.1.3 Peraluminous granite 21

5.2 Geochemical interpretations for the various granites 22

5.2.1 Effects of fractionation on the granites 22

5.2.2 Tectonic settings 23

5.2.3 Evaluation of the mafic enclave relationship with the Walter Outalpa granite 23

5.3 Geochemical comparison with other South Australian Proterozoic granitoids 24

5.3.1 Comparison across the Willyama Supergroup 24

5.3.2 Comparison with the Gawler Craton and Mt Painter Granitoids.24

5.5 Summary 25

CHAPTER 6

ISOTOPE GEOLOGY

6.1 Isotopic results 26

6.2 Conclusion 27

CHAPTER 7

EVOLUTION OF GRANITE GENERATION AND DEFORMATION FOR THE CENTRAL EASTERN WEEKEROO INLIER.

7.1 Magma generation and migration 29

7.2 Regional deformation of the Walter Outalpa granite 30

7.3 Subsequent magma intrusion and deformation 32

CHAPTER 8

CONCLUSION 34

APPENDIX A GEOCHEMICAL ANALYTICAL TECTNIQUES

APPENDIX B ISOTOPE ANALYTICAL TECHNIQUES

CHAPTER ONE:
INTRODUCTION

The Olary Domain contains surface exposures of Proterozoic Willyama Supergroup basement inliers surrounded by Adelaidean rocks. Within the basement are intrusive bodies of Proterozoic age. In order to obtain a better understanding of the regional geological evolution in the central, eastern Weekeroo Inlier, a series of these intrusive bodies were studied. By looking at the timing and method of emplacement of these granites, speculation on the events leading up to and post dating emplacement is possible. Using geochemistry and isotope data, further speculation on the petrogenesis of the granites will be presented. Combining the timing and source of the granites, results in a basis for a model of tectonic setting and evolution of the area during the Palaeo to Mesoproterozoic.

1.1 Review of literature

1.1.1 Problem of timing of granitic emplacement in gneissic terrain.

In gneissic terrains problems with determining the relative timing of granitoid emplacement are increased. Poly deformation cause complicated foliation and contact overprinting. This, with the problem that all granitoid emplacements (pre, syn and post tectonic) can cause similar foliation contact relationships (Paterson et al. 1989), urged the author to explore for microscopic overprinting structures. Variation in pluton composition, fluid/rock interactions and strain rates, will develop similar foliation patterns across pluton wall rock contact (Paterson et al. 1991). Continuity between magmatic to parallel tectonic foliations is the best evidence for syn-tectonic granitoid emplacement (Schofield and D'Lemos 1998). However, no one line of evidence should be used.

1.1.2 Correlating and classifying granitoids

The most common classification of granitic rocks is in terms of mineralogy and/or chemistry, eg two mica granite or peraluminous granite. This method uses measurable and non-genetic parameters. Other methods have a chemical-tectonic approach (Pearce et al., 1984) and magma source compositions inferred using chemical and mineralogical features (Chappell and White 1992). These methods use chemical signatures as being indicative of tectonic environments or source regions. Genetic classifications are unclear when studying more

felsic granites, because these rocks tend to be close to a near minimum-temperature melt composition. Therefore these granites have converging major element compositions and mineral compositions. Fractionation will have a similar effect on the trace element composition, for example fractionated I- and A-type granites will yield similar geochemical signatures (King et al., 1997).

A problem arises when correlating granites. Do similarities between compared granites correlate them or do they relate to a common magmatic evolution or source? Isotope geology is able to distinguish between these two possibilities because magmatic processes do not fractionate isotopes (Rollinson 1993).

1.2 Aims and Methods

The aims of this study are to present an in-depth geochemical and isotopic analyses and detailed mapping of the granitoids and surrounding Willyama metasedimentary country rock within the central part of the eastern Weekeroo Inlier. From such a study, timing relationships between magmatic emplacement and regional deformation, chemical characteristics, granite types and the petrogenesis will be evaluated. It will be determined whether spatially separate granitoids are correlatives and grouped accordingly.

Field mapping was performed using aerial photographs enlarged from 1:25 000 to 1:10 000. Mapping techniques appropriate to gneissic terrains were used, such as form surface mapping (Hobbs et al. 1976).

The major and trace element chemistry of samples was determined using X-Ray Fluorescence analysis (XRF) at the University of Adelaide and Neutron Activation Analysis (NAA) at Becquerel Labs Sydney (Appendix A). Neodymium and strontium isotope ratios were determined using Finnigan Mat 261 and 262 Mass Spectrometers at the University of Adelaide (Appendix B).

CHAPTER TWO:
REGIONAL GEOLOGY

The Olary Domain is located in central eastern South Australia and contains surface exposures of Palaeoproterozoic Willyama Supergroup as basement inliers within Neoproterozoic Adelaidean metasediments and overlying Cainozoic sediments of the Murray Basin (Forbes 1991). Due to the Olary Domain's proximity to the Broken Hill silver-lead-zinc deposits it has been the subject of a number of previous investigations. These prior studies are summarised in this chapter.

2.1 Geological Setting

The semi-isolated outcrops of the Willyama Supergroup have fault contacts with Adelaidean sediments to the west and southwest and an onlapping relationship to the east. Various authors including Stevens et al. (1990) have drawn lithological and stratigraphic correlations between Willyama Supergroup within the Olary Domain and the adjacent Broken Hill Domain (Fig 2.1). Based on a general fining upwards of sediments Willis et al. (1983) interpreted the Willyama Supergroup to represent deposition in a failed Palaeo- to Mesoproterozoic rift. These were subsequently deformed and cratonised. Similar interpretations by Glen et al. (1977) correlated Palaeoproterozoic metasedimentary sequences in the Gawler and Olary domains and inferred that they represented shallow water sedimentation onto older (presumably Archaean) crust. It is interpreted that more distal facies lie to the east.

2.2 Stratigraphy

Detailed lithological studies of the Willyama Supergroup include work by Clark et al. (1986) and Cook and Ashley (1992) from which five conformable rock suites have been determined. Lithological summaries include those of Flint and Parker (1993) and Ashley et al. (1997) and are summarised from oldest to youngest as follows:

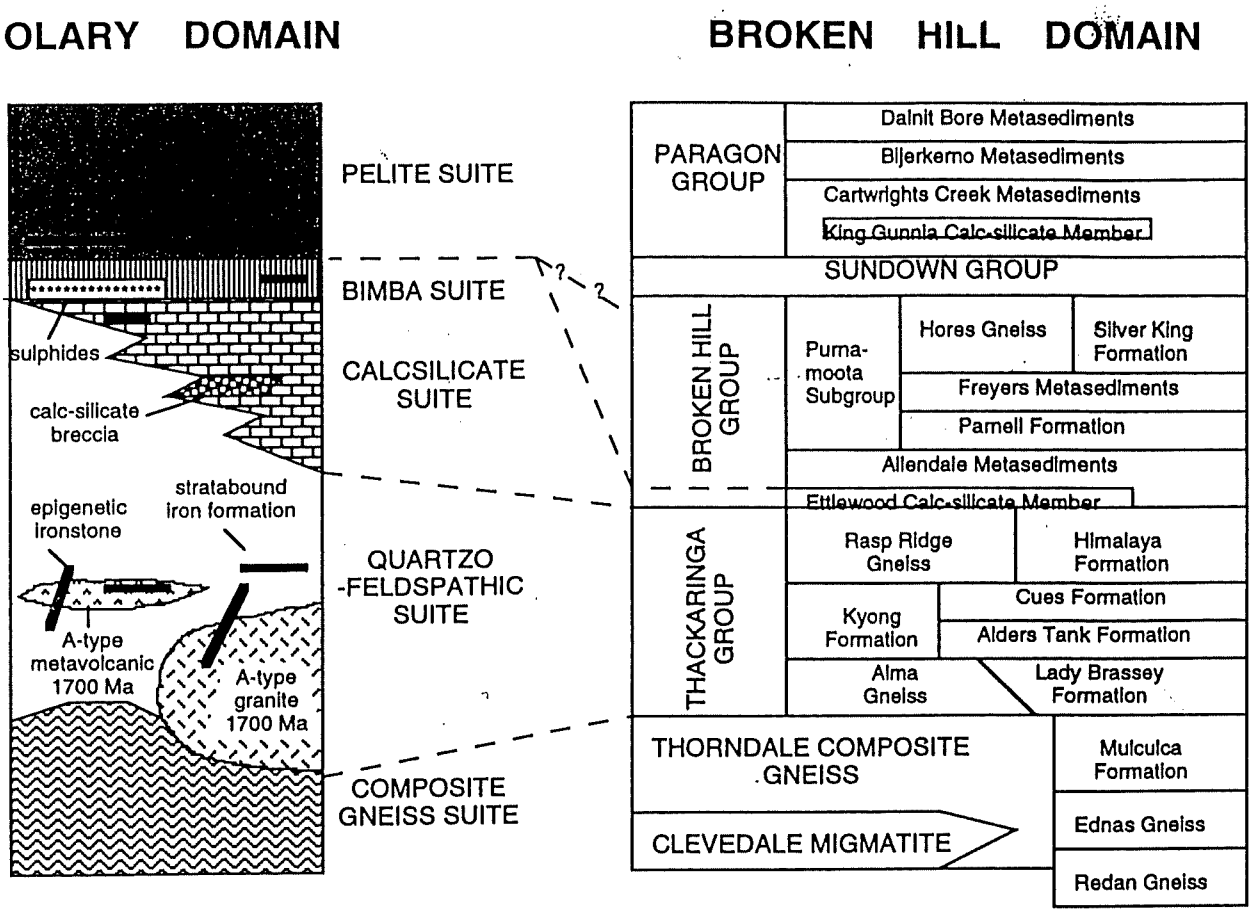

Figure 2.1 Interpreted correlation of the Willyama Supergroup sequences in the Broken Hill Domain with that of the Olary Domain (Ashley et al. 1997).

Composite gneiss suite:

The "composite gneiss suite" is interpreted as the basal unit of the Willyama Supergroup. It is characterised by coarse grained and migmatitic quartz + feldspar + biotite ± sillimanite ± garnet gneiss. The gneiss contains a gradation between psammopelitic and pelitic schists, and quartzofeldspathic members. This gneiss is probably largely metasedimentary in origin, composed of primary psammopelitic sediments, while coarse grained quartzofeldspathic components may have an intrusive origin.

Quartzofeldspathic gneiss suite:

The "quartzofeldspathic gneiss suite" is characterised by irregular layering of quartz + albite + biotite ± K feldspar. The presence of sedimentary structures such as graded bedding, low angle ripple cross laminations and ball and pillow structures plus the presence of pelitic schistose horizons demonstrate a sedimentary environment. Large leucocratic granitic gneiss bodies ranging from massive to foliated types and metavolcanics, recognizable by the presence of quartz eyes, also occur within this suite.

Calcsilicate suite:

The "calcsilicate suite" is characterised by actinolite, diopside and epidote with minor carbonate and fine to thick laminations. The presence of magnetite distinguishes it from the overlying "Bimba suite". Ashley et al. (1997) interpret the depositional environment to be a sabkha-like evaporite.

Bimba suite:

This unit has a gradational contact with the "calcsilicate suite". The "Bimba suite" grades from psammopelitic and pelitic schists into laminated calcsilicate-rich rocks with marble and albite-quartz units. Flint and Parker (1993) suggest that this formation represents a shallow-water, mixed carbonate-pelite unit in a transitional environment between the underlying evaporitic and overlying deep marine units.

Pelite suite:

The "pelite suite" is dominated by pelitic and psammopelitic schists with a typical mineralogy of biotite + muscovite + quartz ± Al silicates ± garnet ± tourmaline. Carbonaceous mica schists passing into pelitic schists with interbedded quartzofeldspathic metasilts mark the basal unit of the "pelite suite".

Separating the Willyama Supergroup from Neoproterozoic metasediments of the Adelaidean Supergroup is the Grand Unconformity of Mawson (1912). The Adelaidean rocks include the Burra and Umberatana Groups that are less deformed than the Willyama basement and of a lower metamorphic grade (lower biotite facies).

2.3 Igneous Activity

Significant igneous activity throughout the Olary Domain is responsible for the presence of regional granitoids and pegmatites. The earliest igneous event formed A-type granitoids (and comagmatic rhyolite volcanics and epiclastics) at about 1700 – 1710 Ma (Ashley et al. 1996). When deformed and metamorphosed these intrusives appear as foliated to massive leucocratic granitic gneisses.

A suite of later S-type (Bimbowrie of Benton (1994)) granitoids that are equigranular, leucocratic, pink to buff coloured and biotite and muscovite bearing intrude the A-type granitoids. This massive to foliated intrusive type is the most extensive intrusive suite throughout the Olary Domain and are informally termed the "regional granitoids" (Flint and Parker 1993). Zircon U-Pb dating has given an age of about 1590 Ma (Cook et al. 1994) for this suite.

A relatively mafic granitoid suite also has surface exposure in the Olary Domain. These are granodioritic to monzogranitic, have I-type affinities and have been dated by Cook et al. (1994) at about 1630 Ma using the zircon U-Pb method.

Pegmatites within the Olary Domain have been interpreted as having developed during high-grade metamorphism and are contemporaneous with the "regional granitoids" (Flint and Parker 1993). Mineralogically they contain microcline + quartz ± sodic plagioclase ± muscovite ± tourmaline. Mineralization includes uranium, thorium and rare earth elements, beryl, rutile, magnetite and iron manganese phosphate minerals (Lottermoser and Lu 1994).

Amphibolites, with a plagioclase + hornblende ± clinopyroxene ± ilmenite ± garnet assemblage, some containing relict igneous textures and minerals, have both conformable and cross cutting relations with their host rocks. Similar metadiorite dykes occur within the Broken Hill Domain and correlations have been drawn by Cowley and Flint (1993) with the Gairdner Dyke Swarm, which have an emplacement age around 827 ± Ma (Wingate et al. 1998).

2.4 Deformation

The Willyama Supergroup has undergone two orogenic events, the Olarian Orogeny at about 1600 Ma and the Delamerian Orogeny at about 500 Ma. The earlier event reached a much higher metamorphic grade and produced more pervasive tectonic fabrics than the latter. The Delamerian had little tectonic influence on the older tectonic fabrics. The Olarian Orogeny has been subdivided to three deformations OD_1-OD_3 and the Delamerian Orogeny into two DD_1 and DD_2 by most authors. Summaries of the Olarian deformations include Flint and Parker (1993) and Ashley et al. (1997). Detailed studies include work by Clarke et al. (1986) and Berry et al. (1978). Table 2.1 shows a summary of tectonic foliations and folding put

TABLE 2.1. Summary of tectonic structures and deformations of various models for the Willyama Supergroup in the Olary and Broken Hill Blocks.

This Study	Berry et al. (1978).	Clarke et al. (1986)	Marjoribanks et al. (1980)
D_3: Retrograde shearing (Greenschist Facies) S_3: Orientated muscovite growth within more pelitic units varying from planar to crosscutting S_1.	**D_3: Folding and retrograde greenschist conditions.** S_3: strong mesoscopic crenulation cleavage in more pelitic units. Has redistributed S_1 and S_2. Muscovite crystallized axial planar to F_3.	**D_3: Retrograde Shear Zones (lower amphibolite – greenschist facies).** S_3: pre-existing fabrics rotated to parallel with generally steeply south dipping strongly foliated zones. F_3: near vertical E striking axial surface. Restricted to discrete shear zones.	**D_3** S_3: vertical axial planar schistosity. A result of crenulated older fabrics and retrograde orientated growth of muscovite and chlorite ± biotite.
D_2 F_2: open to tight folds plunging NE	F_3: open ENE plunging macroscopic folds ($60^0 - 070^0$).	**D_2** S_2: near vertical axial plane defined by moderate to strong crenulations of S_1 (producing a L_2). F_2: meso to macroscopic, upright to reclined, open to tight folds with steeply NW dipping axial surface. Folds trending NE to E.	F_3: small to large scale moderately open folds.
	D_2 S_2: locally weak crenulation restricted to pelitic units concentrated at 120^0. F_2: open local folding.		**D_2** S_2: localized to F_2 hinge zones. F_2: plunge SW at moderate angles parallel to L_1.
D1: Amphibolite Facies S_1: strong schistosity defined by biotite and felsics parallel to layering (bedding)	**D_1: Mid amphibolite facies.** S_1: Schistosity and gniessosity parallel to layering and remnant bedding. F_1: rare mesoscopic isoclinal folds. Syn tectonic granodiorite intrusion.	**D_1** S_1: previously shallow to flat lying axial surface defined by micaeous minerals. L_1: mineral elongation at high angle to fold axes. F_1: meso to macroscopic, tight to isoclinal recumbant folds trending NE to E.	**D_1** S_1: well defined schistosity parallel to bedding. L_1: $30\text{-}35^0$ to the SW F_1: NE closing synforms SW closing antiforms
			Pre S_1 static metamorphism.

"S_n" relates to secondary foliation and its generation.
"L_n" is the lineation generation.
"F_n" relates to tectonic folding and its generation.
"D_n" is the deformation generation.

forward by various authors including the work of Marjoribanks et al. (1980) from within the Broken Hill Domain.

Various structural models have been put forward for the Broken Hill and Olary Domains including:

Model 1 (Clarke et al. 1986).

This model describes north-south-trending nappes of an OD_1 origin. The nappes are refolded in a coaxial manner about upright OD_2 folds whose formation coincided with amphibolite metamorphism. The transport direction for OD_1 is interpreted to be southeastward. Figure 2.2 shows an example of such a model. Laing (1996) proposed a similar model for the Broken Hill Domain.

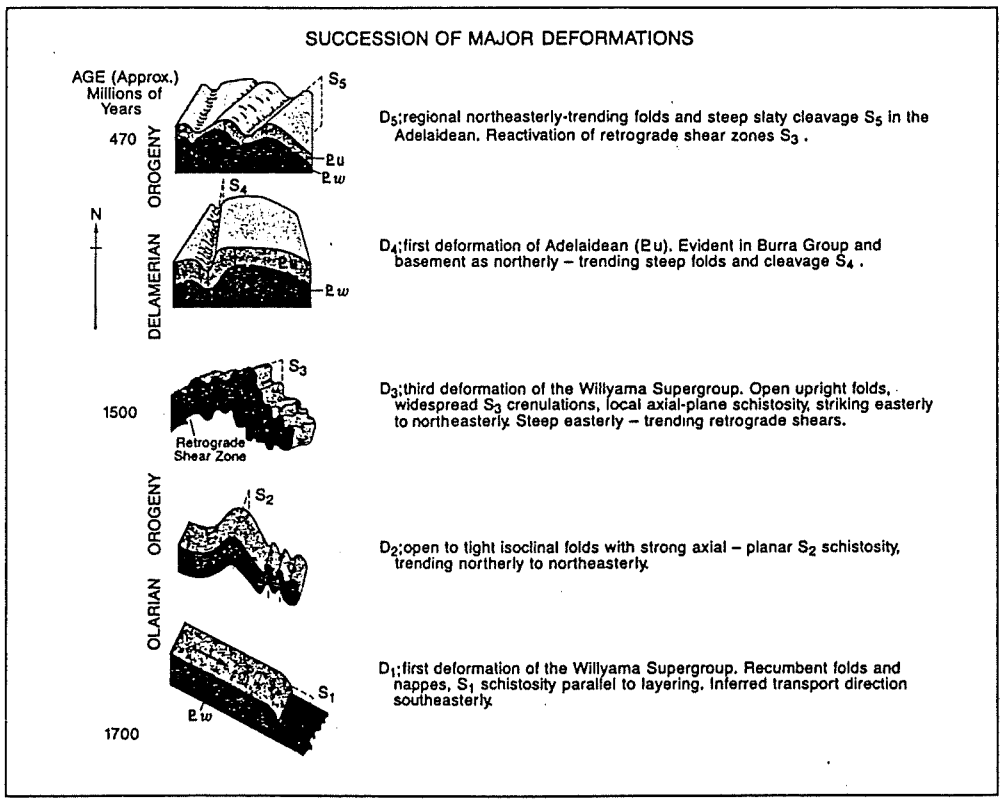

Figure 2.2 Succession of major deformations in the Olary Domain (Forbes 1991).

Model 2 (White et al. 1995).

A second model interprets the Broken Hill Domain as a series of discrete thrust packages separated by high temperature shear zones. The now retrogressed shear zones are interpreted as much older thrusts formed during high-grade metamorphism in the Olarian Orogeny. This model explains the stratigraphic repetition due to high temperature shear zones rather than nappe formation but also predicts a southeast tectonic transport direction.

2.5 Metamorphism

The metamorphic history of the Olary Domain is summarised by Flint and Parker (1993) and Ashley et al. (1997) while detailed studies were undertaken by Clarke et al. (1987) and Clarke et al. (1995). These papers support a general north to south increase in metamorphic grade consistent with that found in the Broken Hill Domain. The metamorphic grade is interpreted as lower to upper amphibolite facies (Fig 2.3). Clarke et al. (1987) used timing relationships between different aluminosilicate polymorphs, overprinting parageneses and peak metamorphism to produce an anticlockwise pressure temperature path for the Olarian Orogeny (pressure increasing with cooling from the metamorphic peak).

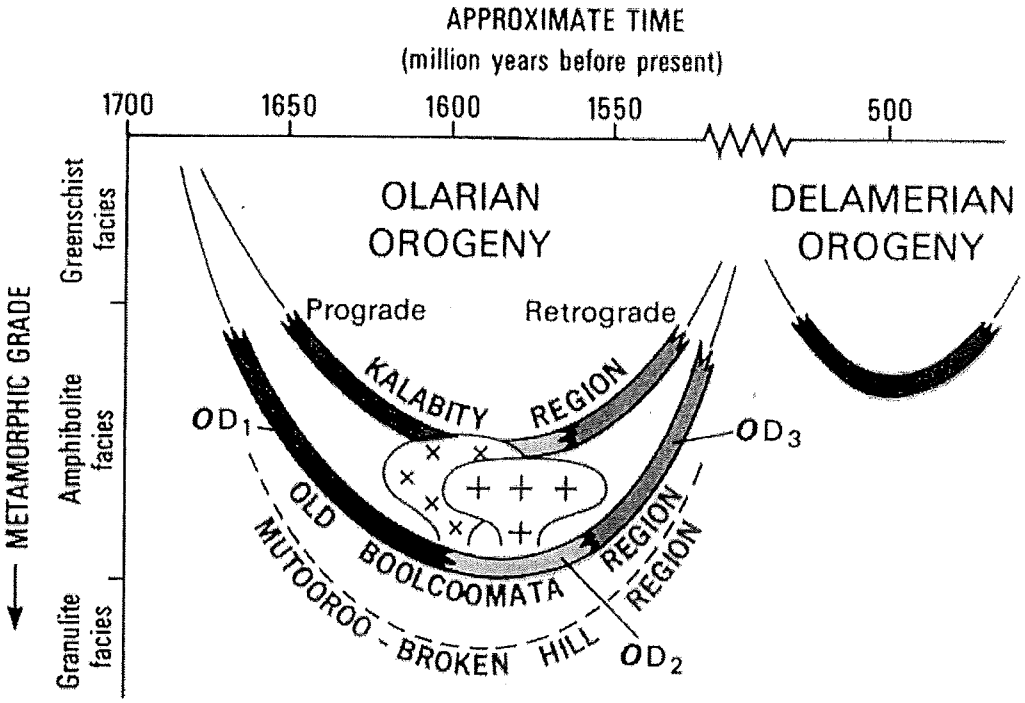

Figure 2.3 Approximate timing and metamorphic grade of tectonic events during the Olarian and Delamerian Orogenies (Flint and Parker 1993)

Retrograde shear zones within the Olary Domain are well defined and are generally east-west striking with steeply south dipping foliations. These zones display recrystallisation of mineral fabrics to lower amphibolite – greenschist facies (Clarke et al. 1986). Steeply plunging lineations have been used to determine a transpression movement with a south over north component.

CHAPTER THREE: LITHOLOGICAL VARIATION WITHIN THE GNEISS COMPLEX OF THE CENTRAL EASTERN WEEKEROO INLIER

Previous detailed mapping of the central Eastern Weekeroo Inlier includes work by Tilley (1990) who mapped the study area at 1:10 000 scale. Clarke et al. (1995) includes a geological map partly covering the study area and Laing (1995) has produced maps including the area at 1:100 000 summarising previous Honours projects in the Olary Domain. However, from previous studies little information was gathered to aid relative timing of the intrusion of the Walter Outalpa granite. This chapter summarises field and petrological observations of the granitic bodies and surrounding metamorphic rocks. The lithological relationships are shown in figure 4.1.

3.1 Metasediments

3.1.1 Layered gneiss

The layered gneiss outcrops around the granitoids in the study area as a thin unit varying from 50 to 400 metres in outcrop width. The layered gneiss unit is dominantly a psammopelitic rock grading from well-layered psammitic and pelitic units, varying from 5 to 50 mm thick (Plate 1.a), into localised migmatic units when close to the Walter Outalpa Shear Zone (Fig 4.1). The melt phase of these thin migmatitic layers is dominantly quartzofeldspathic. Grain size varies across layers from coarse to medium grained. Occasionally inverse metamorphic grading was noticed in outcrop and thin section, and interpreted to represent original younging. Within this unit a tectonic foliation (S_1) is parallel to the primary layering (S_0) display meso to microfolding. Minor phases include magnetite ± muscovite ± monazite. This unit correlates with the "quartzofeldspathic suite" of Clarke et al. (1986).

Within this unit major hematite + barite + quartz pods also occurred both north and south of the Walter Outalpa granite. These range from 10 to 50 metre wide ellipsoidal pods, which outcrop as topographic peaks reaching ten metres above the otherwise undulating terrain.

Plate 1

a) Layered gneiss (1106-025) showing aligned biotite (S_1) parallel to layering. Layering defined by psammitic pelitic alternations. (GPS E:409124 N:6437633)

b) Cross polar photomicrograph of albitite (1106-054). Quartz eyes in fine grained quartz plagioclase matrix suggest a volcanic origin. Opaques are primary magnetite and pyrite. (GPS E:409575 N:6439510)

c) Undeformed Walter Outalpa granite (1106-050) containing white feldspar dominantly plagioclase, translucent quartz phenocrysts and the mafic phase is dominantly magnetite with minor biotite. (GPS E:407185 N:6438778)

d) Cross polar photomicrograph of undeformed Walter Outalpa granite illustrating graphic texture (intergrowths of quartz into feldspar (plagioclase)). Undulose extinction is also illustrated in quartz grains.

e) Surface exposure of mafic enclave. Plagioclase and quartz phenocrysts standout from mafic (biotite) groundmass.

f) Cross polar photomicrograph of mafic enclave (1106-012). Phenocrysts are quartz and plagioclase. The biotite texture is prominently irregular or flow like but, shows some minor alignment. Phenocryst inclusions are biotite. Finer quartz crystals show incipient grain reduction. (GPS E:409959 N:6438850)

g) Hand sample (1106-033) of peraluminous granite. Mafic minerals are biotite. The finer grained felsic minerals are quartz and feldspar. (GPS E:409730 N:6437185)

h) Cross polar photomicrograph of peraluminous granite (1106-033). K feldspar is present as microcline. Both biotite and muscovite are present.

Plate 1

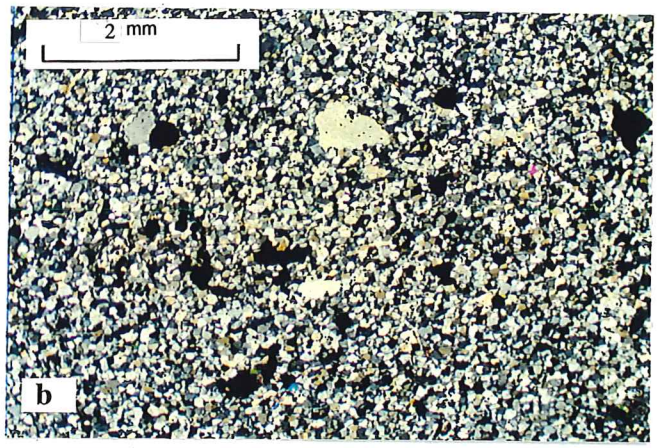

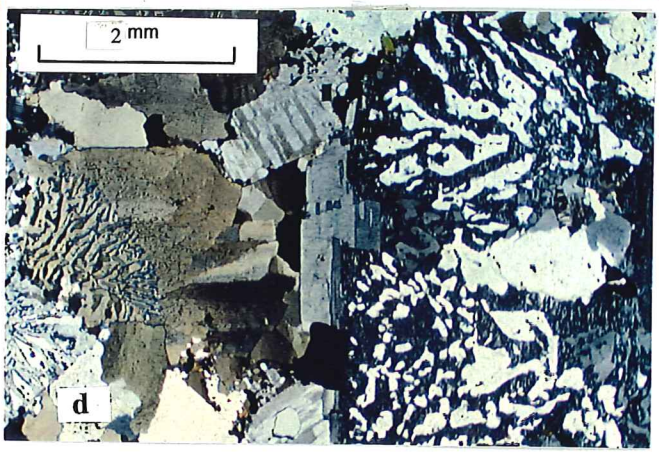

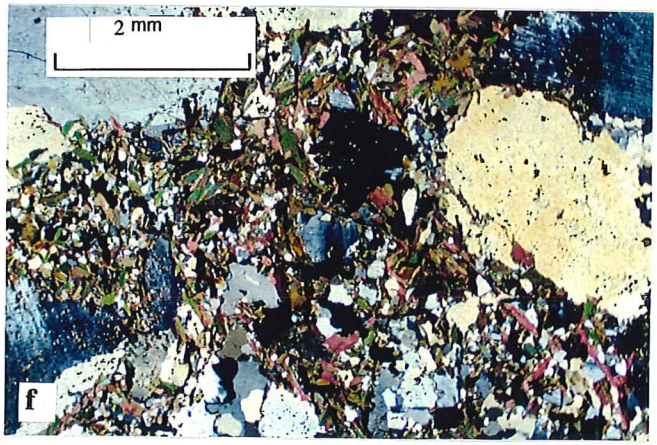

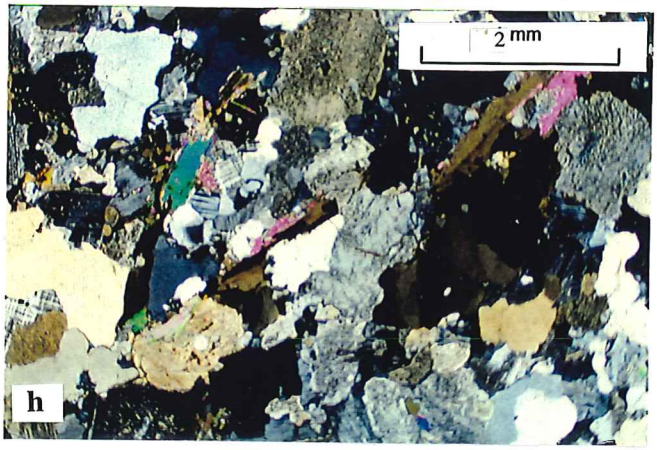

3.1.2 Migmatite Unit

A coarse grained psammitic and pelitic migmatitic unit is restricted to the southern side of the Walter Outalpa Shear Zone. This unit is medium to coarse grained with compositional layering varying in thickness from a few centimetres to tens of centimetres. The coarse biotite and muscovite-rich melanosome are separated by boudinaged and folded leucosome. These mesoscale structures are evident throughout this unit.

3.1.3 Andalusite schist

An andalusite schist is restricted to the northwestern region of the mapped area where its contact is distinct but conformable with the layered gneiss. The mapped thickness of this unit is consistent throughout at approximately 400 metres. It is characterised by andalusite porphyroblasts, which now appear as relict retrograde muscovite. This schist is readily distinguishable in the field due to the presence of these porphyroblasts, which retain their shape. Within this unit, a gradation occurs from muscovite-rich schist with minor andalusite porphyroblasts to schist containing prominent andalusite porphyroblasts. The andalusite schist is a combination of the mica schist and andalusite schist of Clarke et al. (1995). It correlates with the "pelite suite" of Clarke et al. (1986).

3.1.4 Calcsilicate

The calcsilicate unit extends to the edge of the northwestern end of the mapped area and has a conformable contact with the andalusite schist. The calcsilicate unit contains a strong compositional layering defined by cream coloured quartz + feldspar (albite) layers alternating with dark green actinolite + diopside + epidote up to tens of millimetres thick. A preferred orientation of elongate calcic-minerals defines a tectonic foliation parallel to the compositional layering. This unit is correlated with the "calcsilicate suite" of Clarke et al. (1986).

3.1.5 Albitite (meta-rhyolite)

A thin concordant layered albite rich rock outcrops within the layered gneiss and the migmatite units. It is discontinuous within the metasediments north and northwest of the Walter Outalpa granite contact (Fig 4.1). The albitite classification is based on the dominance of albite in weathered and altered (albitised) outcrop where it appears cream and red in colour. However, fresh rock displays quartz eyes suggesting a volcanic or epiclastic origin (Plate 1.b) (Vernon 1986). The quartz phenocrysts are up to 5mm in diameter with the matrix dominated by quartz and feldspar. Oxides are prominent with magnetite abundant, totalling up to 25% of

the rock. Both magnetite and pyrite appear to be primary. The petrology of this unit is consistent with that of the "quartz eye" bearing quartzofeldspathic gneiss of Ashley et al. (1996).

3.1.6 Sheared gneiss

The sheared gneiss is a medium grained psammopelitic unit restricted to the Walter Outalpa Shear Zone. There is very little compositional variation within this unit. Its mineralogy is typically quartz + feldspar + biotite + muscovite + sericite. M domains and aligned microlithon minerals in a seriate polygonal texture define a strong fabric.

3.1.7 Quartz augen gneiss

This unit is related directly to, and contained within, the Walter Outalpa Shear Zone. It is dominated by quartz augen and less common feldspar augen. Typically the quartz augen are 0.5 to 10 mm in length surrounded by pelitic M domains. Characterised by this strong anastomosing tectonic fabric, it is distinguishable from sheared Walter Outalpa granite.

3.2 Intrusives

3.2.1 Walter Outalpa granite

This granitic body makes up the largest proportion of the study area. In the field, weathered outcrops appear as boulders and rounded surfaces on hillsides. Usually it is either a light grey to pink orange in colour with resistant quartz phenocrysts standing out on weathered surfaces. The magmatic mineralogy is homogeneous. It comprises quartz + plagioclase + potassium feldspar (including occasional microcline) + magnetite + pyrite + biotite ± fluorite. Closer to the Walter Outalpa Shear Zone secondary biotite becomes prominent. Quartz phenocrysts from five to ten millimetres in diameter (Plate 1.c), are characteristic of this unit and clearly distinguish it from the otherwise similar peraluminous granite unit. Graphic texture (Plate 1.d) is common (although more strongly deformed samples do not show such a texture). Typically this granite is medium to coarse grained varying from seriate polygonal to inequigranular interlobate. Mineralogy is consistent with the leucocratic medium grained quartz-feldspar unit ("Type B" quartzofeldspathic gneiss) of Ashley et al. (1996). It has previously been named the Walter Outalpa Granodiorite (Belperio 1996).

Mafic enclaves are present within this granite and they typically consist of biotite + plagioclase + quartz ± potassium feldspar ± orthoamphibole ± zircon ± sphene. The extent is shown in figure 4.1. In outcrop the white phenocrysts of plagioclase and quartz have a higher relief than the mafic phases (Plate 1.e). The texture is cumulate-like with biotite surrounding the quartz and plagioclase phenocrysts in both an orientated and irregular fashion (Plate 1.f). The biotite appears to be secondary. Biotite inclusions are present within the phenocrysts. Some quartz and feldspar crystals display grain size reduction to a granoblastic texture.

The eastern and western Walter Outalpa granite sheets have a mapped thickness of 300 to 700m and are truncated by the Walter Outalpa Shear Zone. They outcrop on low lying, undulating hills as bounders and rounded surfaces. These intrusives contain quartz phenocrysts, which are surrounded by finer feldspars (dominantly plagioclase). Other phases include magnetite + biotite + zircon ± muscovite ± fluorite in a granoblastic to inequigranular polygonal texture. Thus these sheet like intrusives have the same mineralogy as the Walter Outalpa granite and hence the three bodies are interpreted as one intrusive.

A third granitic sheet west of the map area but still within the central part of the eastern Weekeroo Inlier (Fig 3.1) outcrops within creek beds. Biotite is the prominent mafic mineral sparsely distributed in surrounding medium to coarse grained granoblastic quartz + feldspars. Minor fine grained magnetite is also present. The aligned biotite forms a tectonic foliation. The mineralogy and texture differ from the Walter Outalpa granite.

3.2.2 Peraluminous granite

The peraluminous granite is situated north of the Walter Outalpa Shear Zone in the central part of the study area. In weathered outcrop it appears pale red with surface exposures typical of granitic terrain consisting of quartz + plagioclase + potassium feldspar + muscovite + biotite ± magnetite. Typically this unit is a medium to fine grained, inequigranular, massive to foliated (Plate 1.g and 1.h). Its texture varies from granitic to gneissic in both thin section and hand sample. This unit has a similar mineralogy to the Bimbowrie granites of Benton (1994). However, it does lack feldspar phenocrysts.

A compositionally and texturally similar rock unit outcropping in the central part of the central Weekeroo Inlier (E:400357 N:6434444) was sampled for comparison with the peraluminous granite. It has a medium grained inequigranular interlobate texture containing dominant microcline and muscovite. Other phases include plagioclase, biotite and minor magnetite. No tectonic fabric was noticed in thin section or outcrop.

3.2.3 Pegmatite

Pegmatites typically dominated by quartz + potassium feldspar + muscovite intrude and crosscut all mapped units. Their size varies from metres to tens of metres long and several metres wide. Their orientation also varies giving an irregular appearance. Within the Walter Outalpa granite they vary from linear to schlieren in outcrop shape, while in the metasediments they are either layer parallel and cross cutting.

3.2.4 Amphibolite

This medium to fine grained unit in outcrop appears massive. The north northeast trending amphibolite dyke consists of amphibole + biotite + quartz + plagioclase + magnetite. Clinopyroxenes and possibly olivine are present as amphiboles.

3.3 Magnetics of the central eastern Weekeroo Inlier

As described above the Walter Outalpa granite has a relatively high percentage of magnetite (5 to 15%). The magnetic susceptibility was also measured at various localities throughout the study area with the Walter Outalpa granite having high readings (0.006 to 0.04). This distinguishes it from the low magnetic susceptibility readings (0 to 0.002) of the peraluminous granite.

This difference is illustrated by the Broken Hill Exploration Initiative regional magnetics (Fig 3.1). The high magnetics of the Walter Outalpa granite depicts a fold like geometry. Note the third granitic sheet (west of the map area) has a much lower magnetic intensity. Line spacing is 100 m.

Figure 3.1

CENTRAL EASTERN WEEKEROO INLIER AIRBORNE TOTAL MAGNETIC INTENSITY MAP

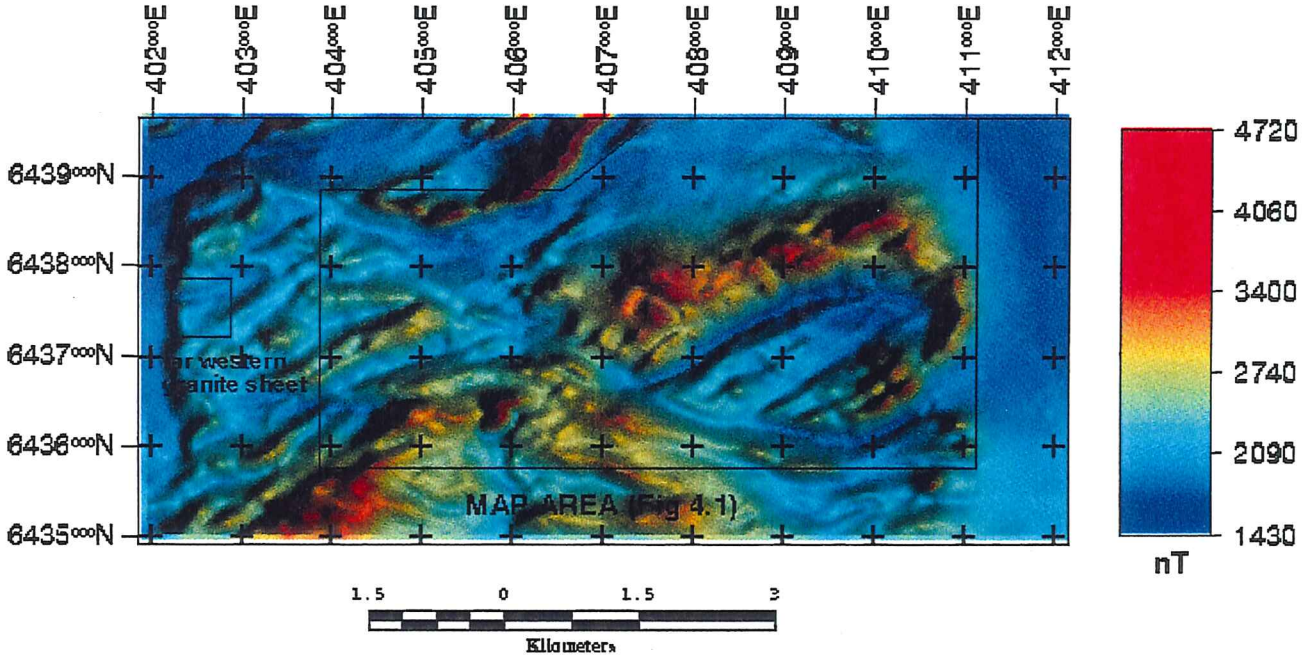

CHAPTER FOUR:
STRUCTURAL DESCRIPTION OF GNEISS COMPLEX, CENTRAL EASTERN WEEKEROO INLIER

The following is a description of the structural observations made on the gneiss complex of the central eastern Weekeroo Inlier. They are the local observations, which have been summarised and correlated with previous work in Table 2.1.

4.1 Foliations

4.1.1 S_0/S_1 in metasediments

Within the more psammitic units, and in particular within the layered gneiss, grain size and mineralogical gradation define a primary sedimentary layering (S_0). In certain locations this gradation was inferred to represent graded bedding enabling determination of younging direction (Plate 2.a). Parallel to this layering is a secondary foliation defined by biotite and aligned microlithons of quartz, K feldspar and plagioclase (S_1) (Plate 1.a). This creates a continuous to spaced, rough layer parallel fabric (S_1) and an equigranular polygonal texture. Clearly recrystallisation and grain size reduction has occurred to create such a mature texture. The absence of undulose extinction in the psammitic minerals supports this. In more pelitic units such as the andalusite schist, continuous parallel mica layers define S_1. The orientation of S_1 is consistent with that in the layered gneiss unit. The orientation of the prominent S_0/S_1 foliation is illustrated in figure 4.1.

4.1.2 S_2 in metasediments

An axial planar cleavage is locally developed in one parasitic fold (Plate 2.b). This foliation cross cuts the earlier S_1 fabric within the layered gneiss trending easterly (088^0) with a vertical dip. The fabric is defined by biotite and has been identified by other workers (see Table 2.1).

Crenulations and a crenulation cleavage are present within the andalusite schist, which have a similar orientation to the parasitic folds within the layered gneiss (see chapter 4.2). Hence they may be of the same generation.

Plate 2

a) Inverse metamorphic grading in layered gneiss interpreted to represent younging (direction of pencil). Layers grading from psammite to pelite are then truncated by psammite. This cycle is repeated. Example located west of northwestern Walter Outalpa granite contact.

b) Parasitic F_2 fold within layered gneiss north of Walter Outalpa granite. Folding contains axial planar foliation defined by biotite in more pelitic layers ($088^0/90^0$).

c) XZ section through deformed Walter Outalpa granite (1106-059). Magnetite and minor biotite make up the mafic phases. Plagioclase and quartz are the felsic minerals.

d) Cross polar photomicrograph of deformed Walter Outalpa granite (1106-047). Recrystallisation and grain reduction of quartz and feldspar overprints relict graphic texture. Opaques present are pyrite and magnetite. (GPS N:408457 E:6437998)

e) Cross polar photomicrography of XZ section of deformed Walter Outalpa granite (1106-059). Grain reduction of quartz is demonstrated. Both quartz and feldspar make up fine grained granoblastic surroundings. Quartz crystal at extinction has biotite tails illustrating dextral movement. Inclusions in quartz grain are biotite.

f) Refolded isoclinal fold within layered gneiss unit north of the Walter Outalpa granite. Illustrates a type three refolded isoclinal interference pattern (Ramsey and Huber 1987). S_1 is folded around open F_2 folds which trend 046^0 and plunge 71^0.

g) Parasitic F_2 fold south of the Walter Outalpa granite. Layer parallel foliation is folded around "Z" shaped fold. Fold axis 73^0-017^0. (GPS E:409124 N:6437633)

h) Hinge associated with major F_2 antiform trending 026^0 plunging 30^0 in the layered gneiss unit north of the Walter Outalpa granite.

Plate 2

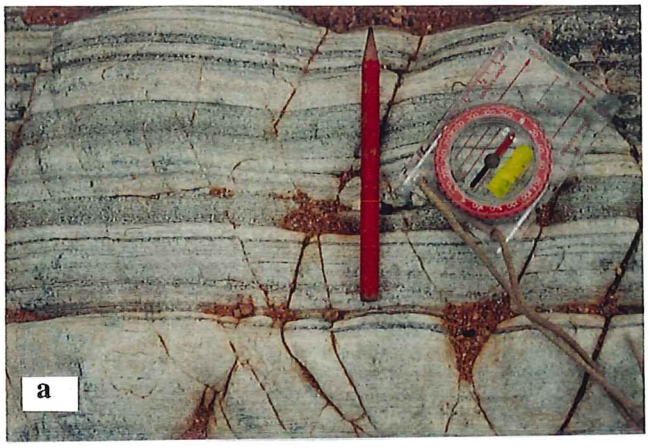

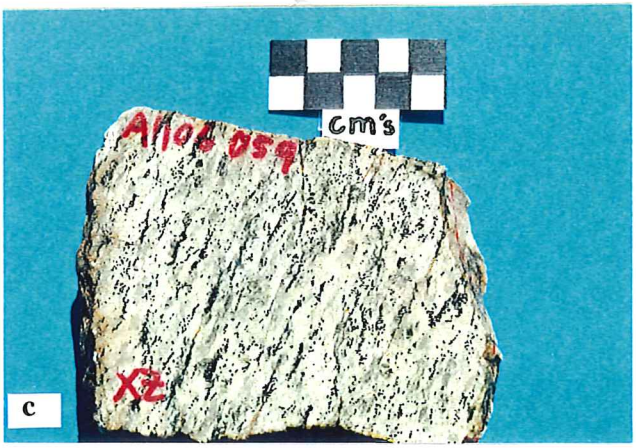

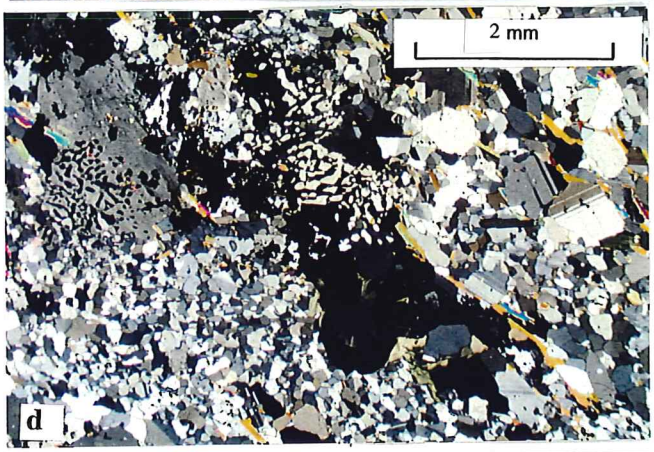

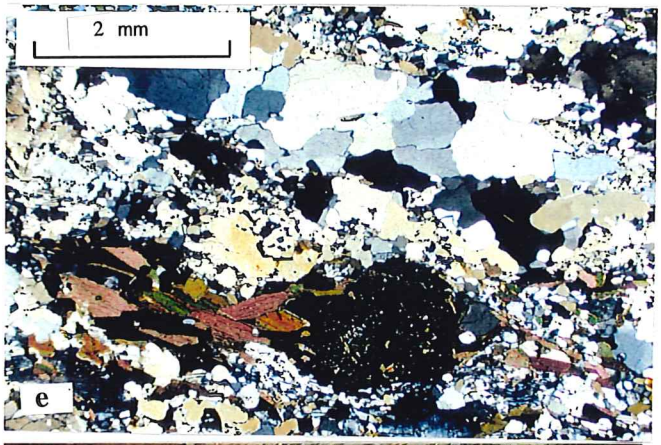

4.1.3 S_3 in metasediments

A retrograde foliation defined by aligned muscovite varies in orientation from parallel to the S_1 fabric to cross cutting S_1. Texturally this fabric is spaced, rough, and has a dextral relationship when cross cutting the prominent S_1 fabric. The general trend of S_3 is 040^0 with a vertical dip. Crenulations of S_3 may relate to a later deformation (Delamerian).

4.1.4 Foliation in the Walter Outalpa granite

The Walter Outalpa granite contains a tectonic foliation defined by magnetite + biotite and aligned quartz phenocrysts (Plate 2.c). This fabric varies in intensity from strong to absent and may relate to strain partitioning typical of granitic bodies (Paterson et al. 1989). Quartz ribbons with undulose extinction, evidence for incipient grain reduction; and the presence of recrystallised quartz and feldspar layers imply temperatures well below the rheological critical melt percent of Tribe and D'Lemos (1996), within a low temperature solid state deformation zone. Where the fabric is strong it has recrystallised the graphic texture (Plate 2.d). This timing relationship suggests a tectonic overprinting event after emplacement, crystallisation and cooling.

Both the western and eastern Walter Outalpa granite sheets display a more granoblastic texture relating to shearing. This effect diminishes away from the Walter Outalpa Shear Zone where quartz phenocrysts become prominent. The quartz phenocrysts are aligned, rounded and form a foliation with magnetite and feldspar.

Graphic intergrowths of quartz and feldspar hide, replace or overprint any pre-rheological critical melt percentage fabrics possibly formed within this granite. Thus, no continuum from magmatic foliation to parallel tectonic foliation (eg Paterson et al. 1989; Paterson et al. 1991) was noticed to support Clarke et al.'s (1986) interpretation that the granite is syn-tectonic. Graphic texture is characteristic of shallow level emplacement (Burnham and Ohmoto 1980).

Subhorizontal mineral lineations within the vertical foliation indicate elongation towards 060. This strike-slip regime contains dextral kinematics (Plate 2.e).

4.1.5 Foliation in the peraluminous granite

There is a foliation in the peraluminous granite, which is defined by aligned biotite creating a spaced rough foliation parallel to elongate microlithons of feldspar and quartz in an inequigranular to seriate interlobate texture. There is a decrease in fabric intensity away from the Walter Outalpa Shear Zone. The more deformed samples show recrystallisation of quartz

Figure 4.1 Geological Map

CENTRAL, EASTERN WEEKEROO INLIER.

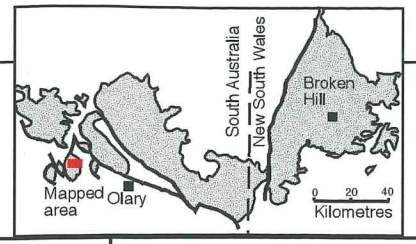

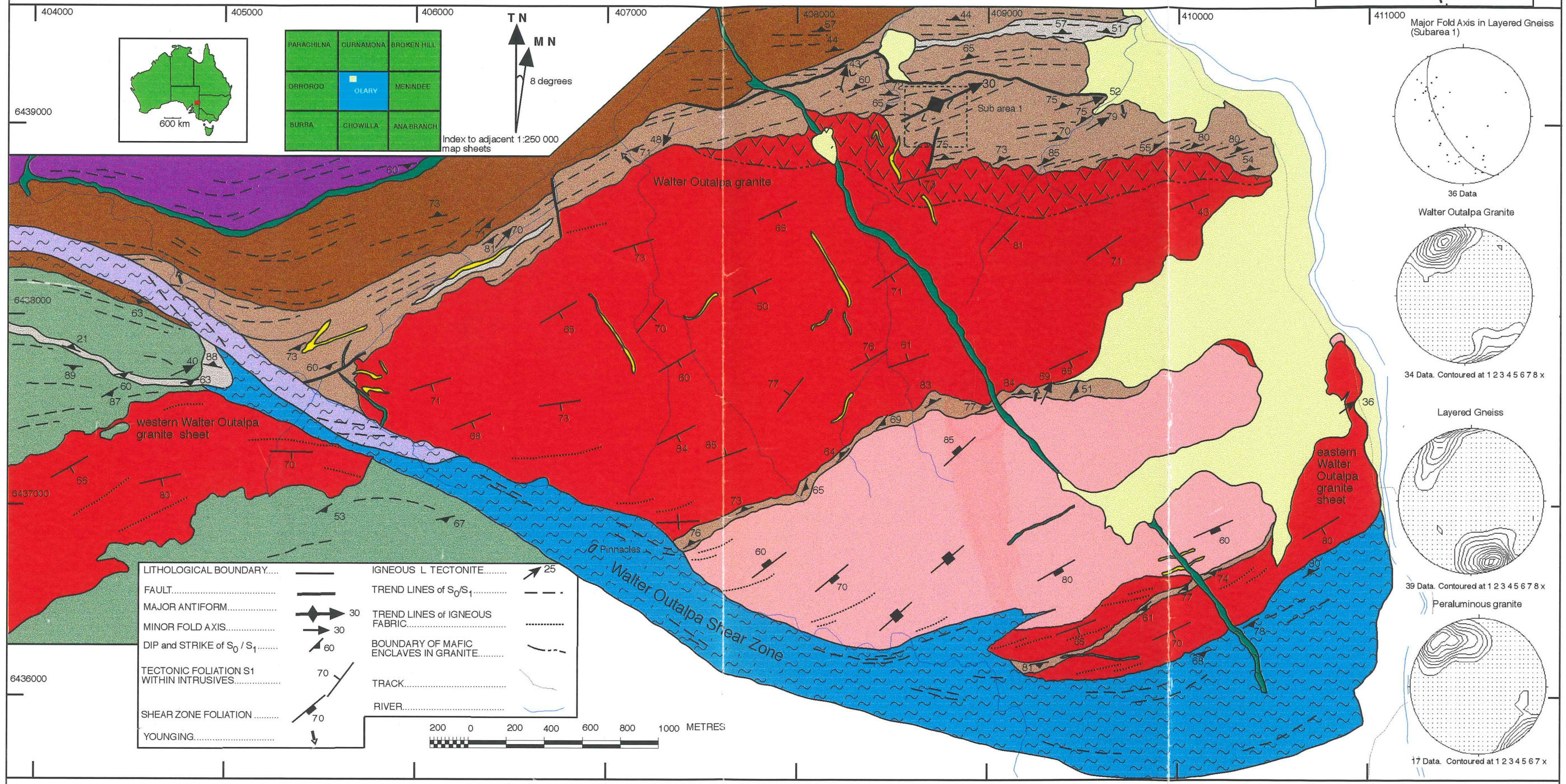

Alluvium

SHEAR ZONE

Quartz augen gneiss:
containing quartz and feldspar augens to 10mm in pelitic anastomosing fabric.

Sheared gneiss:
medium grained, psammopelitic layering with strong layer parallel foliation.. Quartz + feldspar + biotite + muscovite +sericite.

INTRUSIVES

Pegmatite:
coarse equigranular quartz + K feldspar + muscovite.

Amphibolite:
massive equigranular amphibole + biotite + plagioclase + magnetite.

Peraluminous granite:
medium grained inequigranular massive to foliated plagioclase + K feldspar + muscovite + biotite ± magnetite.

Mafic enclaves:
discontinuous mafic enclaves containing quartz and plagioclase phenocrysts in a biotite matrix.

Walter Outalpa granite:
equigranular to inequigranular massive to foliated quartz phenocryst bearing + plagioclase + K feldspar + magnetite ± biotite.

METASEDIMENTS

Calc silicate:
alternating layers of quartz + feldspar, cream layers and actinolite + diopside + epidote as green layers.

Andalusite schist:
coarse grained pelitic unit grading from minor andalusite porphyroblasts to prominent andalusite porphyroblasts within strong schistosity.

Albitite (metarhyolite):
fine grained with laminations dominated by albite and quartz. Quartz eyes are also present.

Migmatite:
has a psammitic, peltic layering with the melt component mainly quartz +feldspar.

Layered gneiss:
medium grained psammopelitic with strong layer parallel fabric quartz + feldspar + biotite + magnetite ± muscovite ± monazite.

Drafted by Damian Brett B. Sc
Department of Geology and Geophysics
University of Adelaide, July 1998.

Australian Mapping Grid SI - 54 - 2.

and feldspar typical of temperatures well below the rheological critical melt percent depicting similar relationship to the Walter Outalpa granite. The fact that the foliation rapidly decreases in intensity away from the shear zone, and contact timing relationships of this unit (see section 4.5) imply that this tectonic foliation was created by the retrograde shearing event (D_3).

The trend and distribution of the two solid state tectonic foliations, in the intrusives, is illustrated in figure 4.1. The respective stereonet plots show a similar orientation for these two fabrics.

4.2 Folding

4.2.1 First generation folds (F_1)

The evidence supporting more than one generation of folding is the presence of refolded folds (Plate 2.f). Here the isoclinal fold is being refolded about the axis 71^0-046^0 of a more open fold. This represents a type three refolded isocline interference pattern (Ramsey and Huber 1987). In this example the tectonic foliation (S_1) is folded around the later open fold axis. Within the more migmatitic lithologies similar fold interference patterns were noticed, however it is the leucosome fraction which is "folded".

4.2.2 Second generation folds (F_2)

These folds are parasitic to major, open to isoclinal folds, trending northeast (Plate 2.g and 2.h). Transposition of psammitic layers within pelitic layers in the layered gneiss is commonly present near such folds. To derive a precise trend of the major F_2 fold axis north of the Walter Outalpa granite, detailed measurements in subarea 1 (Fig 4.1) were made and plotted on a stereonet. This antiform plunges 30^0 towards 062^0. The vergence of the parasitic folds is consistent with the major fold axis mapped north of the Walter Outalpa granite. There is no evidence that such F_2 folds continue into the granites.

One fold within the study area displays an axial planar cleavage (Plate 2.b). It is a tight fold plunging east. Berry et al. (1978) interpret such folds to be of a separate generation (Table 2.1).

4.3 Faulting and shearing

The Walter Outalpa Shear Zone trends northwest southeast across the study area. This shear zone is a dextral, transpressional, steep south-dipping feature (A. Bottrill pers. com. 1998).

Localised shearing is also present on both the northern and southern contacts of the Walter Outalpa granite within the layered gneiss unit. Such shearing is subvertical with a shallow, westerly plunging lineation.

Faulting within the metasediments is present north of the northern Walter Outalpa granite contact where it is interpreted to be post F_2 as it truncates the major fold (Fig 4.1). Faulting which displaces and crosscuts the granite wall rock contact may be related to brittle deformation during emplacement or to an orogenic event. No relationship was observed which would allow the timing of these events to be determined.

4.4 Metamorphism

The mineralogy of the samples studied implies, at peak prograde metamorphism the study area reached amphibolite facies. Evidence for retrograde metamorphism is present in the form of S_3 muscovite growth in the metasediments and muscovite growth within the western granitoid. Other evidence is present within the Walter Outalpa Shear Zone where recrystallisation of mineral fabrics to chlorite and muscovite, and extensive hydration of previous assemblages suggest greenschist metamorphism (A. Bottrill pers. com. 1998).

4.5 Metasediment – Granitoid Relationship

A distinct contact is present along the northern boundary of the Walter Outalpa granite and the layered gneiss. The Walter Outalpa granite wall rock contact truncates the S_1 in the metasediments at an acute angle. However, the presence of the mafic enclaves masks any direct foliation relation across the wall rock intrusive contact. The corresponding foliations do follow a similar azimuth (Fig 4.1 stereoplots).

Along the north western contact of this igneous body, the contact is concordant (Fig 4.2). The metasediment and granite foliations are parallel. This, and the fact that metasediments have a southerly dip imply that either the Walter Outalpa granite was emplaced above the andalusite schist or local overturning has occurred. Local younging and regional stratigraphy imply the latter.

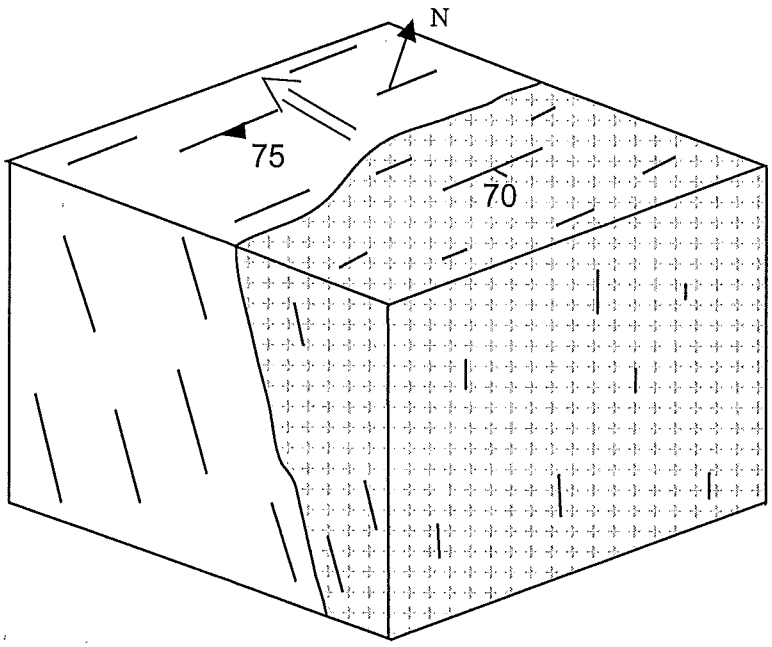

Figure 4.2 Schematic diagram of concordant layered gneiss - Walter Outalpa granite contact. Younging implying overturned orientation. Foliations are consistent in strike and dip.

The southeastern contact is not as distinct and varies from truncating the fabric of the metasediment to a parallel relationship between the metasediment fabric and the igneous contact.

Contact relationships between the Walter Outalpa granite sheets and metasediments are not clear due to the presence of migmatite and the Walter Outalpa Shear Zone. However, the eastern Walter Outalpa granite sheet (Fig 4.1) is in contact with the layered gneiss. Here the granite wall rock contact is concordant and the two tectonic foliations are parallel to each other, trending in a northeasterly direction.

The peraluminous granite truncates the layered gneiss and its tectonic fabric along all its contacts. The fabric within this unit has a consistently different orientation to the layered gneiss (refer to stereonets in figure 4.1). This orientation is similar to that of the Walter Outalpa granites but only dominant near the Walter Outalpa Shear Zone. These timing relationships imply late to post D_2 emplacement.

4.6 Discussion on the timing of the Walter Outalpa granites

The evidence presented above implies that the gneiss complex of the central eastern Weekeroo Inlier has undergone at least two Mesoproterozoic deformations. The first deformation produced a layer parallel fabric. This foliation may relate to regional isoclinal folding (Clarke et al. 1986). Another option for creating a layer parallel foliation is subhorizontal shearing (E. Paul pers. com. 1998). Continued deformation or a second distinct deformation folded the earlier fabric. Two discrete deformations is preferred because of the regional evidence for three fold generations, the last of which is seen in the study area. A shear zone represents the final Mesoproterozoic deformation to affect this region truncating all prior tectonic features.

There are two possible options for the emplacement of the Walter Outalpa granite:

- Pre-tectonic (D_1) emplacement
- Post-D_1 but pre-D_2 emplacement

based on the overprinting of crystallisation textures by low temperature solid state deformation textures. A pre-D_1 emplacement is supported by concordant contacts between the wall rocks and the granite. This interpretation is consistent with geochemically similar granites (see chapter five) across the Olary Domain (Ashley et al. 1996). Thus the foliation within the Walter Outalpa granites is contemporaneous with the development of the layer parallel foliation S_1 in the metasediments.

The absence of any folding of the tectonic foliation within the Walter Outalpa granite supports emplacement between D_1 and D_2. In this case the tectonic foliation within the Walter Outalpa granite is S_2 and the same generation as the folding of S_1.

CHAPTER FIVE:
GEOCHEMICAL INVESTIGATIONS

Mapping and petrology has separated the intrusives into lithological units (see chapter three). This chapter aims to compare and contrast their geochemical signatures, to classify the intrusives and to make correlations both within the Olary Region and across Australia's Proterozoic granites.

5.1 Geochemical signature of intrusives

5.1.1 Walter Outalpa granites

The Walter Outalpa granite is chemically homogenous and has a felsic affinity, exhibiting high SiO_2 and low Al_2O_3, MgO, CaO, TiO_2 and P_2O_5 (Table 5.1 and Fig 5.1). The Na_2O/K_2O ratio is very high throughout this unit (Table 5.1). It is depleted in low field strength elements (LFSE) and transition metals (V, Cu, Ni, Zn), while being enriched in the high field strength elements (HFSE) and rare earth elements (REE), in comparison to the Bulk Continental Crust of Taylor and McLennan (1985) (Fig 5.3).

The granite sheets within the map area (eastern and western Walter Outalpa granite sheets (Fig 4.1)) display very similar major element signatures to the above mentioned granite (high narrow SiO_2 range and low Al_2O_3, MgO, CaO, Fe_2O_3T and TiO_2 (Table 5.1)). The eastern Walter Outalpa granite sheet has a very high Na_2O/K_2O ratio and likewise low Ba and Rb values. However, the western Walter Outalpa granite sheet has low Na_2O/K_2O ratios and high Ba and Rb values. Both sheet granites are enriched in LREE and HFSE, while being deplete in Sr and transition metals and thus display very similar immobile trace element geochemical signatures supporting the correlation of these sheets with the Walter Outalpa granite (Fig 5.3).

Aluminium Saturation Index (ASI) (Chappell and White 1992) for the Walter Outalpa granite and associated granite sheets range from 1.0 to 1.07 (Table 5.1) indicating the rocks are metaluminous. The classification diagram (Na_2O + K_2O versus SiO_2, Fig 5.2b (Cox et al., (1979)) places these units in the granite field. This diagram was chosen because it combines both alkalis in an attempt to counter problems with post-emplacement mobility, which may be

Table 5.1

	Walter Outalpa granite							Mafic enclave			WWO granite sheet			EWOGS
GPS	409485	408457	407185	407213	407282	407282	411160	409959	409959	409309		404269	402320	410433
	6438500	6437998	6438778	6438529	6437865	6437865	6436720	6438850	6438850	6438687		6437221	6436700	6436764
Sample Name	1106-039	1106-047	1106-050	1106-051	1106-052	1106-053	1092-T27	1106-012	1106-013	1106-042	1106-001	1106-036	1106-062	1106-048
SiO2 %	76.21	76.34	77.68	77.53	77.79	78.35	78.1	64.90	65.46	67.31	77.23	75.53	75.73	77.14
Al2O3 %	11.08	10.96	11.22	11.51	10.92	11.40	10.22	15.39	13.98	14.02	11.53	11.88	11.17	11.40
Fe2O3T %	4.84	4.24	3.16	2.93	3.79	1.37	3.93	3.13	4.01	2.58	2.22	2.89	4.52	3.64
MnO %	0.01	0.01	0.01	0.01	0.01	0.01	0.01	0.03	0.04	0.04	0.01	0.02	0.02	0.01
MgO %	0.25	0.98	0.51	0.57	0.56	1.16	0.62	5.44	5.98	5.30	0.11	0.20	0.22	0.08
CaO %	0.06	0.12	0.06	0.07	0.09	0.09	0.13	0.20	0.13	1.10	0.28	0.64	0.40	0.09
Na2O %	6.21	5.99	6.22	6.32	5.96	6.11	5.3	6.46	5.34	5.97	3.68	3.37	4.02	6.58
K2O %	0.31	0.39	0.51	0.50	0.40	0.74	0.54	2.93	3.32	2.17	4.30	4.74	2.78	0.10
TiO2 %	0.22	0.23	0.23	0.22	0.24	0.23	0.26	0.34	0.28	0.36	0.13	0.18	0.26	0.24
P2O5 %	0.07	0.02	0.02	0.02	0.01	0.01	0.03	0.02	0.02	0.05	0.01	0.01	0.02	0.03
SO3 %	0.01	0.01	0.01	0.01	0.00	0.01	0	0.01	0.01	0.01	0.01	0.01	0.00	0.00
LOI %	0.06	0.16	0.14	0.13	0.23	0.25	0.28	0.44	0.43	0.67	0.33	0.44	0.28	0.14
Total %	99.33	99.44	99.78	99.81	100.00	99.72	99.41	99.30	99.01	99.57	99.83	99.90	99.42	99.45
Trace elements (ppm)														
Zr	396.2	405.0	437.0	558.6	428.0	507.1	463	564.4	488.1	510.0	300.2	430.9	658.2	357.1
Nb	70.4	68.0	69.0	66.8	61.1	65.4	73	45.2	87.1	61.5	99.2	87.1	57.4	72.4
Y	132.3	134.0	88.8	112.5	150.7	143.0	145.7	122.6	46.0	236.3	113.7	102.1	173.5	74.2
Sr	10.7	11.4	11.7	11.6	13.7	16.9	38	17.4	13.9	22.2	14.9	16.4	41.3	13.4
Rb	32.1	23.6	20.6	17.9	12.3	28.8	17.2	166.1	189.4	108.2	88.2	126.4	61.2	2.8
U	5.7	4.0	17.2	5.8	5.2	4.8	6.8	4.5	6.2	2.8	9.7	10.6	5.7	4.9
Th	24.2	32.8	31.1	33.5	30.6	31.1	37.9	28.2	34.3	20.6	29.7	39.5	29.8	30.5
Pb	8.1	4.7	5.8	7.7	23.7	5.9	14.8	3.0	3.8	3.9	5.3	7.6	8.0	3.0
Ga	30.8	26.4	30.5	29.0	25.8	28.1	26.7	35.5	30.9	24.6	35.3	31.6	24.3	28.3
Cu	28	3	12	4	23	2	16	4	13	2	2	4	4	10
Zn	4	9	5	6	11	6	28	46	70	52	6	20	17	3
Ni	4	5	10	10	9	5	2	106	55	50	3	5	7	5
Ba	15	19	56	26	17	17	525	128	147	130	503	640	1036	20
Sc	3.8	4.4	4.7	4.8	2.1	2.9	2.5	9.5	11.8	5.2	-0.4	1.9	2.6	4.4
Co	6	10	7	8	6	5	77	20	22	12	4	4	5	10
V	3	6	21	15	10	7	13	59	49	31	3	5	4	21
Ce	192	137	168	182	271	116	211	27	68	16	143	174	295	98
Nd	96	81	75	81	134	59	90	12	24	6	53	40	213	71
La	86	67	80	89	119	54	87	8	33	1	83	41	169	33
Cr	127	91	145	113	182	163	0	282	59	60	104	143	139	92
Eu	4.57	3.58	1.92	3.04	3.61	2.40		1.01	1.09	1.26	1.52	0.96		2.61
Hf	20.10	20.80	21.20	23.60	18.20	21.40		24.80	20.00	24.30	19.00	20.00		24.30
Lu	2.54	2.47	1.65	2.04	2.19	2.38		1.96	0.88	3.20	2.10	2.31		1.73
Sm	34.30	22.80	19.90	22.60	35.00	20.50		5.25	6.18	6.27	9.44	9.06		22.20
Ta	2.72	8.78	5.98	7.07	6.39	6.25		7.18	4.66	6.71	6.40	5.19		6.17
Yb	17.60	16.80	11.50	13.70	15.10	16.50		13.30	5.70	23.50	14.50	14.90		12.00
Mag Sus		0.03	0.04	0.02	0.0003	0.0002						0.04		0.035
Na2O/K2O	20.294118	15.478036	12.196078	12.589641	15.088608	8.2679296	9.8148148	2.2032742	1.6074654	2.7524205	0.8568102	0.7106706	1.4481268	68.541667
ASI	1.0397864	1.0447165	1.0299918	1.0399991	1.0504395	1.0349764	1.0713252	1.0865454	1.1080671	0.9895165	1.0283938	1.0033751	1.079747	1.0277727
Zr sat Temp	875.57561	878.90521	884.66533	911.27612	885.91749	900.79524					845.97673	877.6545		863.09025

Table 5.1

	Peraluminous granite				Granitic sheet		Meta-rhy	Amphib	Xenolith	Micropegmatite
GPS	409147	410805	409730	400357	402340	402500	409575			410400
	6437503	6437884	6437185	6434444	6437620	6437700	6439510			6437840
Sample Name	1106-024	1106-028	1106-033	1106-003	1106-060	1106-061	1092-T85	1106-032	1106-002	1106-010
SiO2 %	75.28	74.09	73.76	75.06	74.12	75.00	68.25	49.98	89.07	76.02
Al2O3 %	12.97	14.31	14.46	13.96	12.99	13.06	15.13	14.74	5.53	10.48
Fe2O3T %	1.40	1.50	1.74	1.33	3.27	1.93	5.04	13.98	0.83	6.16
MnO %	0.01	0.01	0.01	0.02	0.01	0.01	0.01	0.29	0.01	0.01
MgO %	1.53	0.40	0.39	0.37	0.47	1.07	0.07	6.35	0.72	0.14
CaO %	0.24	0.29	0.45	0.51	0.63	0.52	0.04	7.61	0.12	0.36
Na2O %	6.43	4.20	5.88	5.03	5.63	6.73	8.88	2.41	2.35	3.93
K2O %	1.08	3.97	2.82	3.09	1.98	0.90	0.23	2.09	0.54	2.08
TiO2 %	0.48	0.14	0.18	0.11	0.35	0.34	0.52	1.49	0.42	0.32
P2O5 %	0.10	0.15	0.15	0.07	0.15	0.12	0.13	0.16	0.04	0.02
SO3 %	0.00	0.01	0.01	0.01	0.00	0.01		0.02	0.00	0.01
LOI %	0.28	0.87	0.33	0.42	0.25	0.36		0.66	0.23	0.44
Total %	99.79	99.93	100.18	99.97	99.85	100.04		99.78	99.86	99.97
Trace elements (ppm)										
Zr	387.0	114.1	173.9	144.6	344.6	352.5		106.8	714.0	506.8
Nb	43.9	34.0	19.6	11.5	45.4	37.6	192.4	9.2	10.5	54.2
Y	104.4	53.9	60.2	71.1	117.6	98.9	18	33.8	36.5	58.8
Sr	22.0	21.0	26.3	33.8	59.2	33.8	211.1	289.7	25.4	48.0
Rb	56.3	255.9	114.5	135.6	61.6	49.3	14.6	130.6	37.1	54.1
U	1.5	13.0	15.8	11.6	4.0	3.3	3.6	0.1	2.7	7.8
Th	25.1	20.8	30.7	36.6	25.6	24.4	6.2	1.1	9.5	17.8
Pb	4.1	10.9	10.1	14.8	8.6	4.8	19.8	34.1	2.2	2.5
Ga	21.9	21.4	18.5	19.5	22.7	21.6	6.3	20.2	6.9	25.4
Cu	2	4	4	3	6	2	24.2	53	1	20
Zn	8	11	10	7	10	11	3	377	4	6
Ni	8	3	4	5	11	11	1	57	8	5
Ba	55	167	170	260	590	132	13	319	79	747
Sc	12.6	11.3	8.2	1.9	10.9	12.5	12	34.5	5.1	8.0
Co	5	3	5	5	7	7	2.2	40	2	8
V	22	12	14	12	7	15	113	397	30	4
Ce	130	33	61	79	170	165	118	37	67	40
Nd	61	12	27	27	89	81	699	11	31	15
La	63	13	29	29	80	78	337	10	34	18
Cr	98	102	104	126	143	116	337	73	141	116
Eu	1.46	0.57	0.70	0.88			55	1.15	1.75	1.70
Hf	15.30	3.85	4.85	5.15				2.52	22.30	19.10
Lu	1.78	0.86	0.92	1.24				0.48	0.56	1.41
Sm	15.20	4.11	6.79	7.96				4.51	11.00	4.55
Ta	5.12	3.66	3.65	2.58				-1.00	2.01	4.43
Yb	12.10	5.84	6.44	8.68				3.24	3.60	8.47
Mag Sus	0.0002	0.003	0.001						0	0.02
Na2O/K2O	5.9758364	1.0576681	2.082153	1.6299417	2.8477491	7.4611973	38.608696	1.1525586	4.3438078	1.8867019
ASI	1.0649796	1.2194734	1.0673428	1.1130563	1.0353165	1.0051651	1.0134171	0.7346607	1.1842555	1.1179681
Zr sat Temp										

Key

western WO granite sheet (WWO granite sheet)
Eastern Walter Outalpa granite sheet (EWOGS)
Meta-rhyolite (Meta-rhy)
Amphibolite (Amphib)

Magnetic Susceptibility (Mag Sus)
Aluminium saturation index (ASI)
Zr Saturation Temperature (Zr sat Temp)

prefix 1092 (Stoian, unpublished data)

associated with these elements. The high Ga/Al and Zr + Ce + Nb + Y, shown on the discrimination diagrams of Whalen et al. (1987) (Fig 5.6a and b) suggest an A-type character.

Variation in Na_2O, K_2O, CaO, Rb and Ba probably relates to a post-emplacement alteration event present in many Olarian intrusives (Ashley et al. 1997). Rare earth elements are less susceptible to alteration events (Rollinson 1993). Rare Earth elements (Fig 5.3) show a strong correlation between both the Walter Outalpa granite and the granitic sheets, suggesting that the differences relate to different degrees of post-emplacement alteration.

The granitic sheet outside of the map area (Fig 3.1) has a geochemical signature, which differs from the Walter Outalpa granite (Table 5.1 and Figs 5.1, 5.2 and 5.3). This sheet (circled in figures 5.1, 5.2 and 5.6) is enriched in TiO_2, CaO, Al_2O_3 and Sr (Table 5.1) relative to the Walter Outalpa granite. It is similar to sample 1106-024 (see peraluminous granite).

All these intrusive bodies resemble the I-type, Sr-depleted, Y-undepleted, enriched in incompatible elements (anorogenic granites) of Wyborn et al. (1992).

5.1.2 Mafic enclaves

The mafic enclaves have high MgO, Al_2O_3, Na_2O and K_2O and relatively low SiO_2 compared with the Walter Outalpa granite (Table 5.1 and Fig 5.1). They are depleted in transition metals, P_2O_5, Sr, Pb and Ba but enriched in Rb. They are also enriched in HFSE, while the light REE display varying and complicated signature (Fig 5.5).

5.1.3 Peraluminous granite

These intrusives are peraluminous with high SiO_2 and Al_2O_3, and low MgO, TiO_2 and CaO (Table 5.1 and Fig 5.1). The Na_2O/K_2O ratio is moderate compared to the other granite in the area (Table 5.1). A geochemical signature similar to bulk continental crust, especially in LREE, is diagnostic of this unit (Fig 5.4). The peraluminous granite is depleted in Sr, transition metals and to a lesser extent Ba, while enriched in Rb, U and Th. They are similar to the S-type granites, Sr-deplete, Y-undepleted of Wyborn et al. (1992).

The chemical variation across these samples may relate to their geographic position with respect to the Walter Outalpa Shear Zone. The sample closest to the shear zone is depleted in mobile elements such as K, Rb, Ba and U, and enriched in the immobile elements Zr, Ti, Y and the LREE. This variation decreases with distance from the shear zone. There is a strong similarity between the closest sample to the shear zone (1106-024) and the samples from the

Figure 5.1

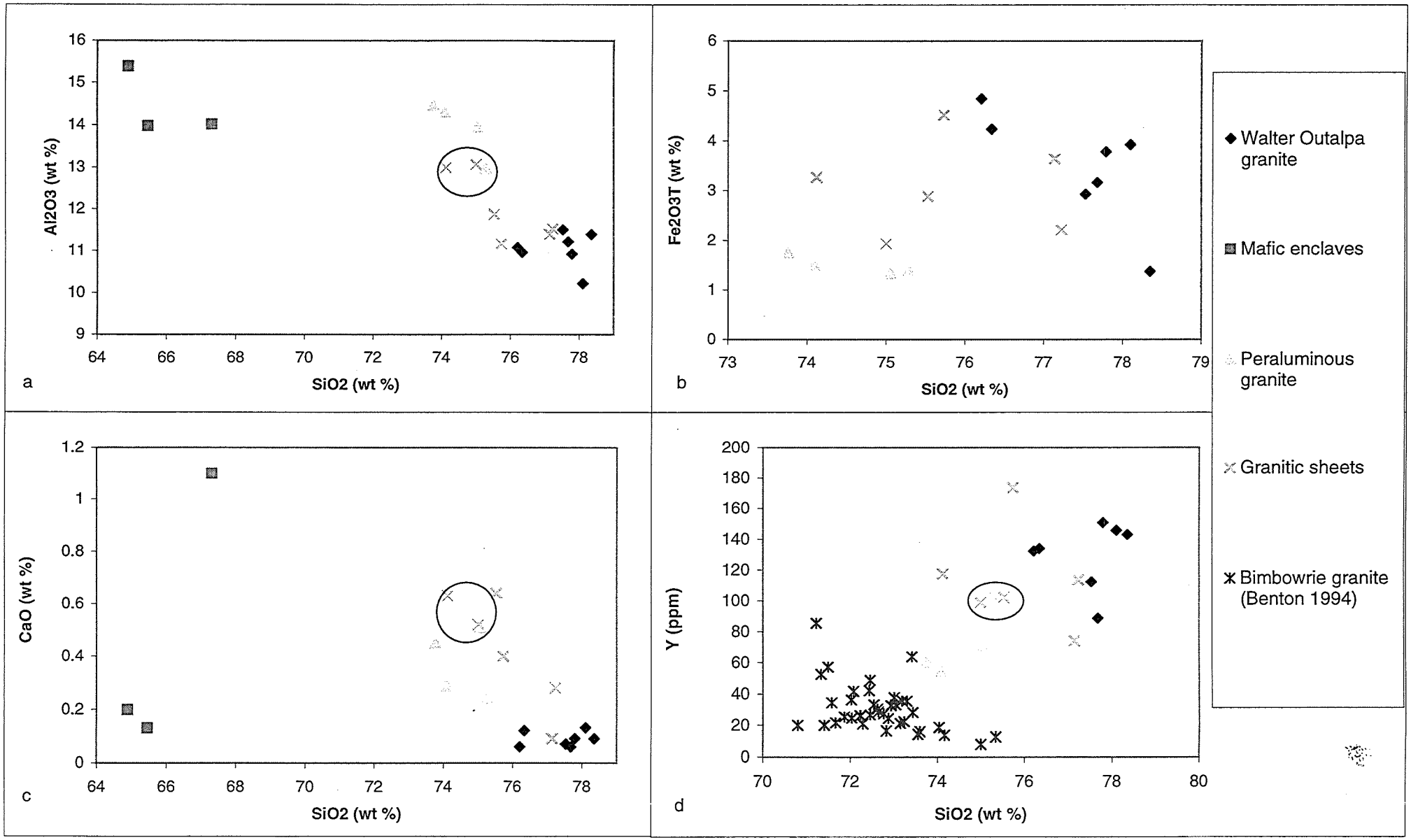
Al2O3 (wt %)
SiO2 (wt %)
a
Fe2O3T (wt %)
SiO2 (wt %)
b
CaO (wt %)
SiO2 (wt %)
c
Y (ppm)
SiO2 (wt %)
d
Walter Outalpa granite
Mafic enclaves
Peraluminous granite
Granitic sheets
Bimbowrie granite (Benton 1994)

Figure 5.2

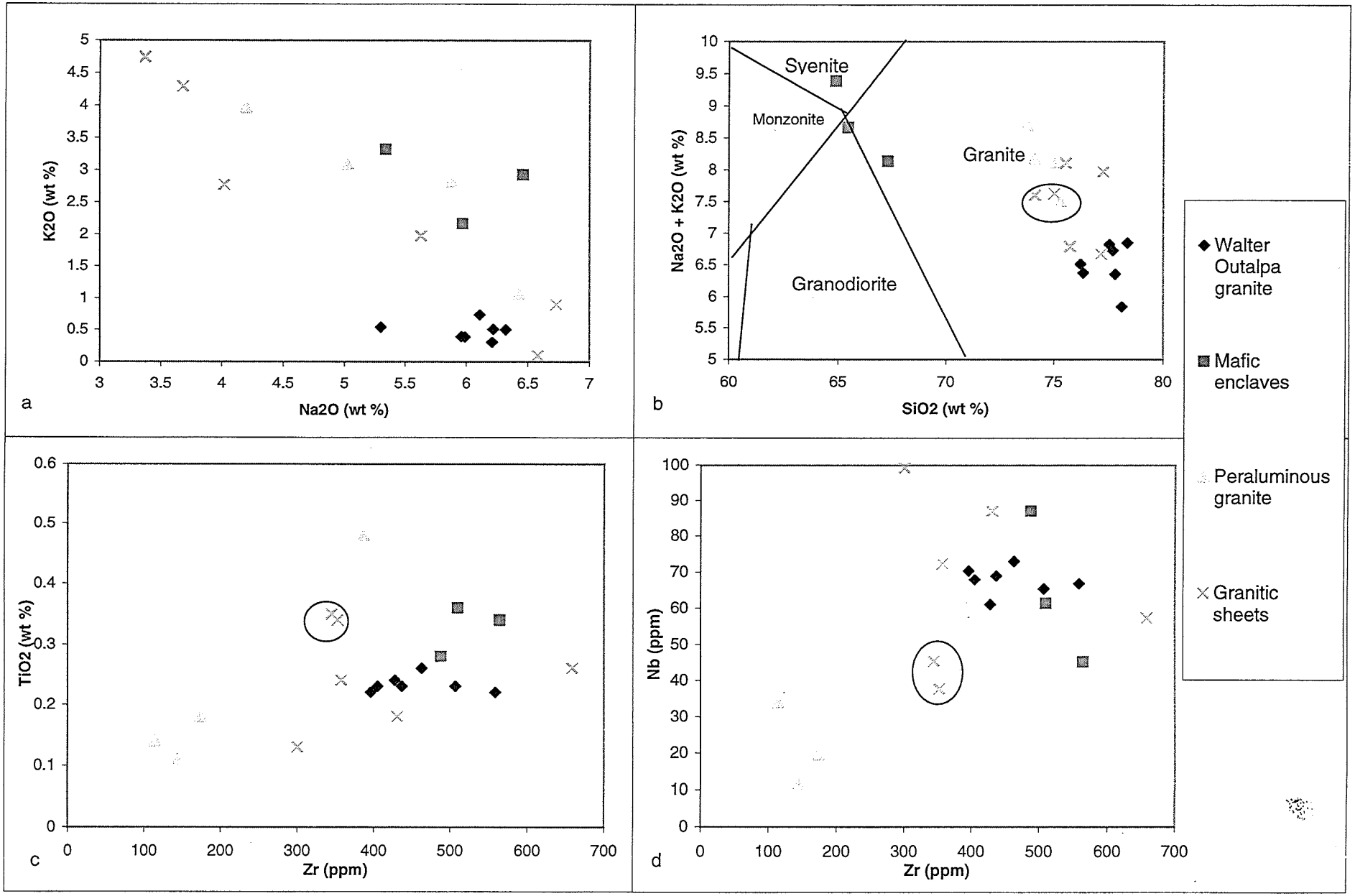
a
K2O (wt %)
Na2O (wt %)
b
Na2O + K2O (wt %)
SiO2 (wt %)
Syenite
Monzonite
Granite
Granodiorite
c
TiO2 (wt %)
Zr (ppm)
d
Nb (ppm)
Zr (ppm)
Walter Outalpa granite
Mafic enclaves
Peraluminous granite
Granitic sheets

far western granite sheet (Fig 3.1). These samples may represent a separate granite unit displaced by the Walter Outalpa Shear Zone. However, lack of samples prevents such a conclusion.

The low Zr + Nb + Ce + Y and Ga/Al and high ASI suggest an S-type chemical affinity. However, samples closer to the Walter Outalpa Shear Zone trend to higher Zr + Nb + Ce + Y and Ga/Al and low ASI values giving a more I-type signature (Fig 5.6a and b).

These above geochemical groupings are consistent with lithologies proposed by field and petrological observations and supported by bivariate and multi element plots (Figs 5.2, 5.3, 5.4, and 5.5).

5.2 Geochemical interpretations for the various granites

5.2.1 Effects of fractionation on the granites

Fractionation processes cause S-, I-, and A-type granites to have similar geochemical signatures. However, some trace elements have varying trends with fractionation within these groupings. For example, Th and Y increase substantially in amount with fractionation of I-type granites, while remain constant for S-type granites (Chappell and White 1992). Increasing P_2O_5 with fractionation is characteristic of S-type, while P_2O_5 remains constant in A-type granites. This makes it possible to distinguish between these granite types. A method for distinguishing between A- and I-type granites is by using the Zr saturation temperature equation of Watson and Harrison (1983). By definition, A-type granites are high temperature melts. The Lachlan Fold Belt granites demonstrate this feature with fractionated A-types having higher temperatures (800^0C) than fractionated I-types (760^0C) (King et al. 1997). This equation uses whole rock geochemistry of granites to calculate their temperatures. If zircon inheritance is present then higher than actual temperatures will be calculated.

Across the Walter Outalpa granites are very high SiO_2, low CaO and Sr implying highly fractionated intrusives. A Walter Outalpa granite correlative at Ameroo Hill has no inheritance (Fanning 1995). Therefore it is assumed the Walter Outalpa granite has no inheritance and elevated temperatures present for the Walter Outalpa granite imply an A-type character.

Figure 5.3

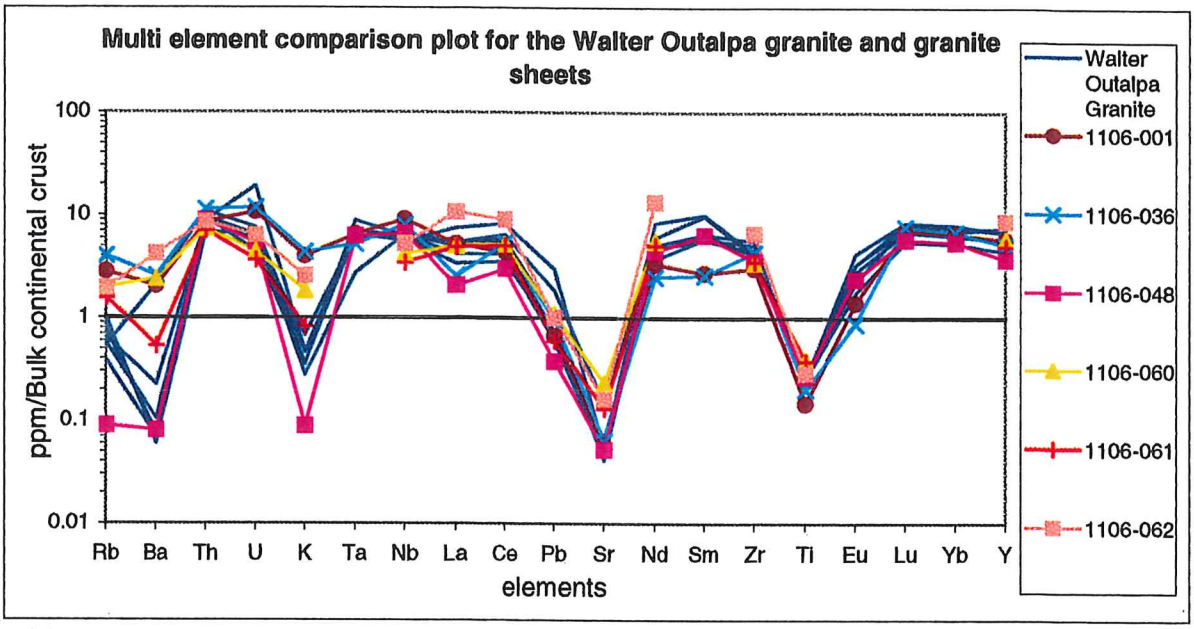

Figure 5.4

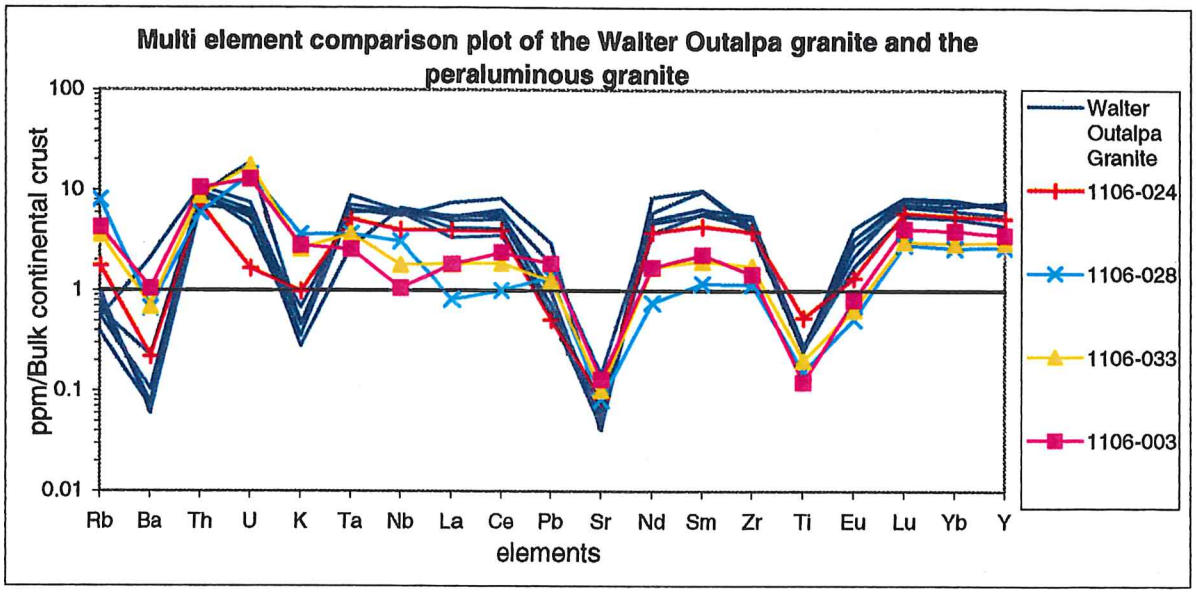

Figure 5.5

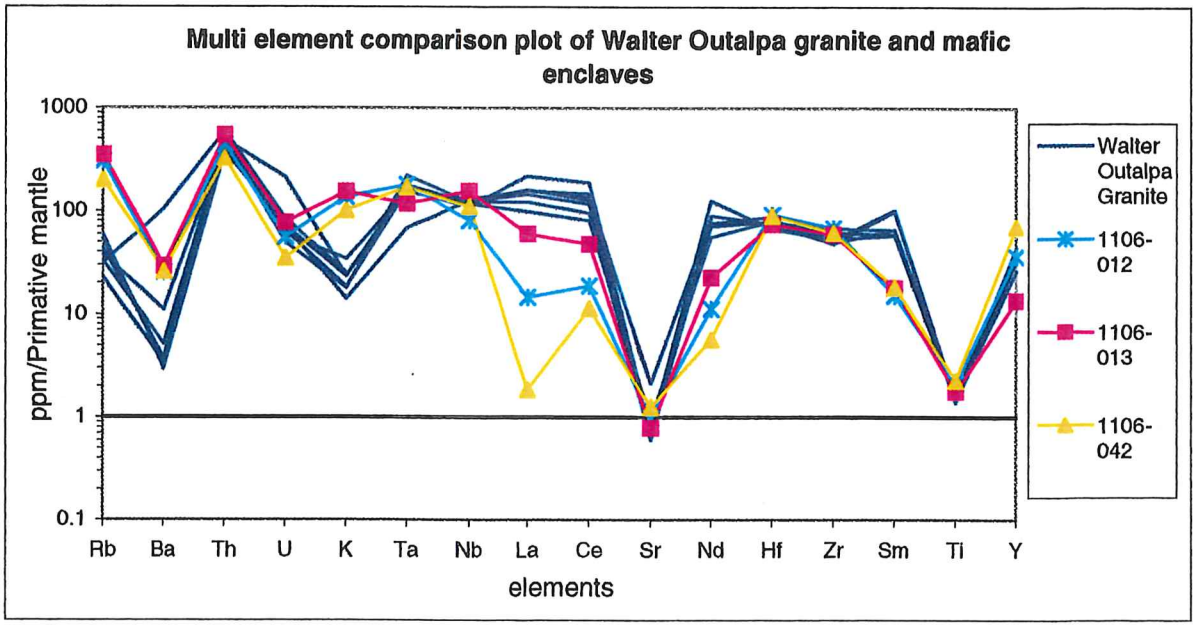

Feldspar, biotite and magnetite have been fractionated in the production of the Walter Outalpa granites. The fractionation of these phases has produced negative Eu anomalies (Fig 5.3), TiO_2 depletions (Fig 5.3) and Fe_2O_3T depletions (Fig 5.1b) respectively. With the removal of biotite, zircon was also fractionated (as inclusions in biotite) as shown by the TiO_2 versus Zr diagram (Fig 5.2c). Hornblende fractionation is responsible for light REE prominence. The fractionation of these phases is source independent.

Trace element data for the peraluminous granite imply that it has been subject to fractionation. A negative Eu anomaly suggests feldspar fractionation. Figure 5.1d shows the peraluminous granite could have an I-type granite trend (increasing Y with fractionation). The few data points for this granite make classification difficult. The Bimbowrie granite has a clear S-type trend.

5.2.2 Tectonic setting

Geochemistry signatures for granites also allow the evaluation of various tectonic settings. The tectonic discrimination diagrams of Pearce et al. (1984) shows that the Walter Outalpa granite plots in the within plate granite (WPG) zone (Fig 5.6c). This is consistent with an A-type character. Figure 5.6d illustrates possible alteration of the Walter Outalpa granite being depleted in the mobile element Rb. A similar result is present for the eastern Walter Outalpa granite sheet having very low Rb causing it to plot within the ocean ridge granite field.

The peraluminous granite also plots within the WPG zone. This illustrates the limiting aspect of using trace element data to classify granites on the basis of tectonic environment. Pearce et al. (1984) assume a mantle component in this granite classification scheme to remove the complexities caused by totally crustal derived melts, which have such a heterogeneous source.

5.2.3 Evaluation of the relationship between the mafic enclave and the Walter Outalpa granite

The mafic enclaves are clearly distinguishable by their geochemistry. However, there are some similarities between the mafic enclaves and the Walter Outalpa granite in trace element abundances, especially the HFSE, suggesting diffusion or mixing between the two units (Fig 5.5). The high K_2O within the mafic enclaves relates to their high modal abundance of biotite with respect to the granites, where K_2O is mostly contained in feldspar.

Theories to explain mafic enclaves include the restite model (Chappell et al. 1987), injection of mafic magma (Wiebe 1996), mafic intrusion and stoping of country rock. Bivariate plots

Figure 5.6 Discrimination diagrams

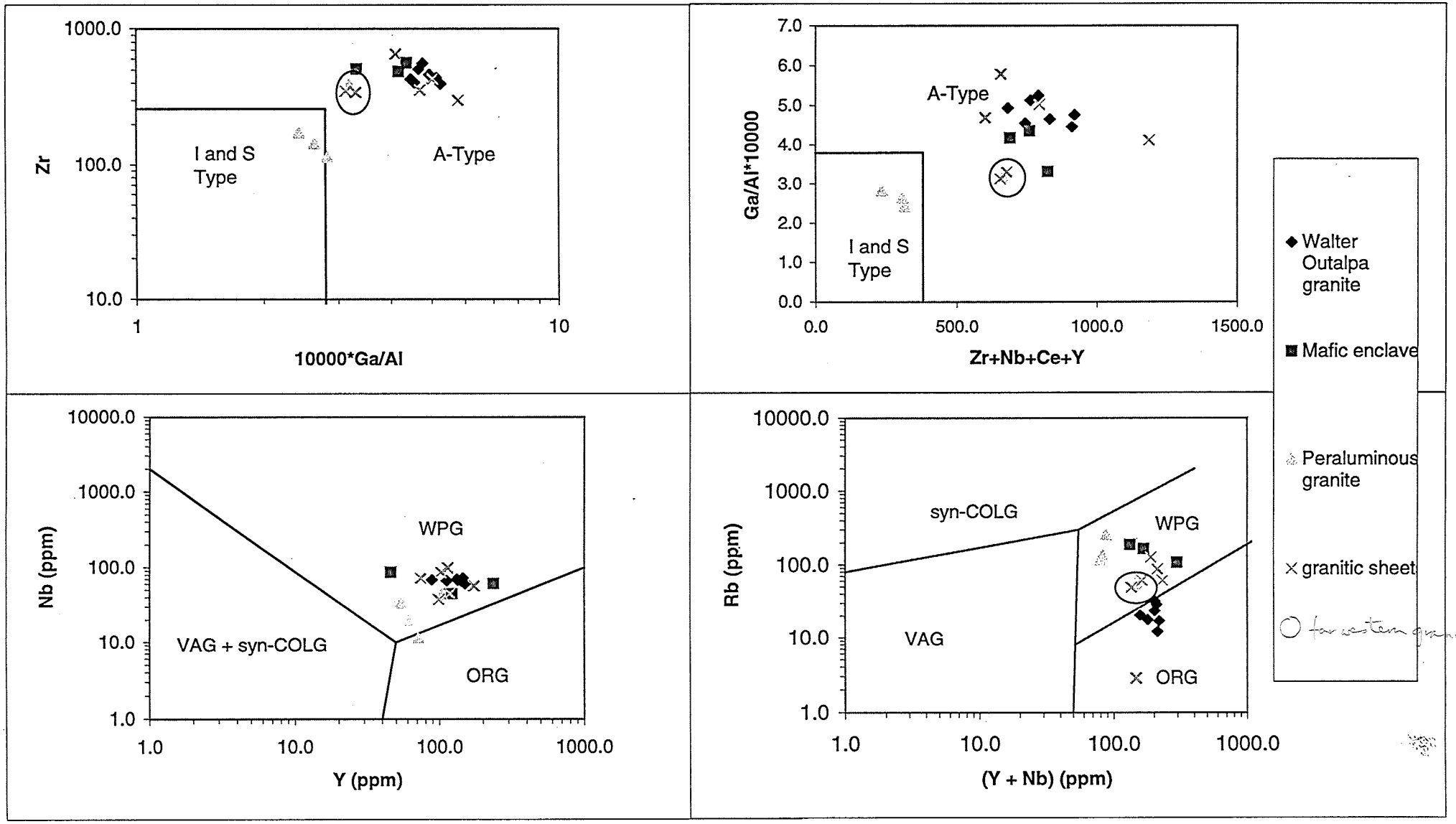

suggest at least some similarities between the enclaves and their host granite due to diffusion or mixing. This does not favour any of the above mentioned models. However, the restite model predicts restite will only be present as dispersed crystals in highly fractionated units (Collins 1998), which may discount the enclaves representing restite. Possible sources for a mafic intrusion include lamprophyres in the Olary Domain (Freeman 1995). However, trace element compositions suggest the mafic enclaves are unrelated to these lamprophyres. The enclaves are restricted to the northern margin of the Walter Outalpa granite, which supports them being formed by stoping of country rock and diffusion between granitic magma and stoped material. This is the preferred explanation.

5.3 Geochemical comparison with other South Australian Proterozoic granitoids.

5.3.1 Comparison across the Willyama Supergroup

Comparisons between with Olary Domain granitoids are illustrated in figures 5.7, 5.8 and 5.9. There is a strong correlation between the metagranitoid of Ashley et al. (1996) and the Walter Outalpa granite (Fig 5.7). Similarly the Walter Outalpa granite resemble the Basso Granodiorite, which is described as an A-type granite (Benton 1994). The Walter Outalpa granites differ from the Antro Granite, which is described as an I-type granite (Benton 1994).

Within the central Weekeroo Inlier are discontinuous meta-rhyolite units (petrographically similar to the albitite unit, see chapter three) with A-type affinities (Szpunar 1997). The meta-rhyolite sample from central, eastern Weekeroo Inlier (1092-T85) correlates with the Walter Outalpa granite supporting a comagmatic relationship (Fig 5.8), although there is some variation in light REE. The samples from the central Weekeroo Inlier (1093-35 and 1093-1) differ and seem to be unrelated.

The S-type of Ashley et al. (1996), the Bimbowrie Granite (Benton 1994) and the peraluminous granite away from the shear zone, show strong similarities (Fig 5.9). This however, may relate to fractionation of the peraluminous granite.

5.3.2 Comparison with the Gawler Craton and Mt Painter Granitoids

Two geographically close Proterozoic domains containing granitoids with A-type characters are the Gawler Craton (K. Stewart University of Adelaide, unpublished data) and the Mount

Figure 5.7

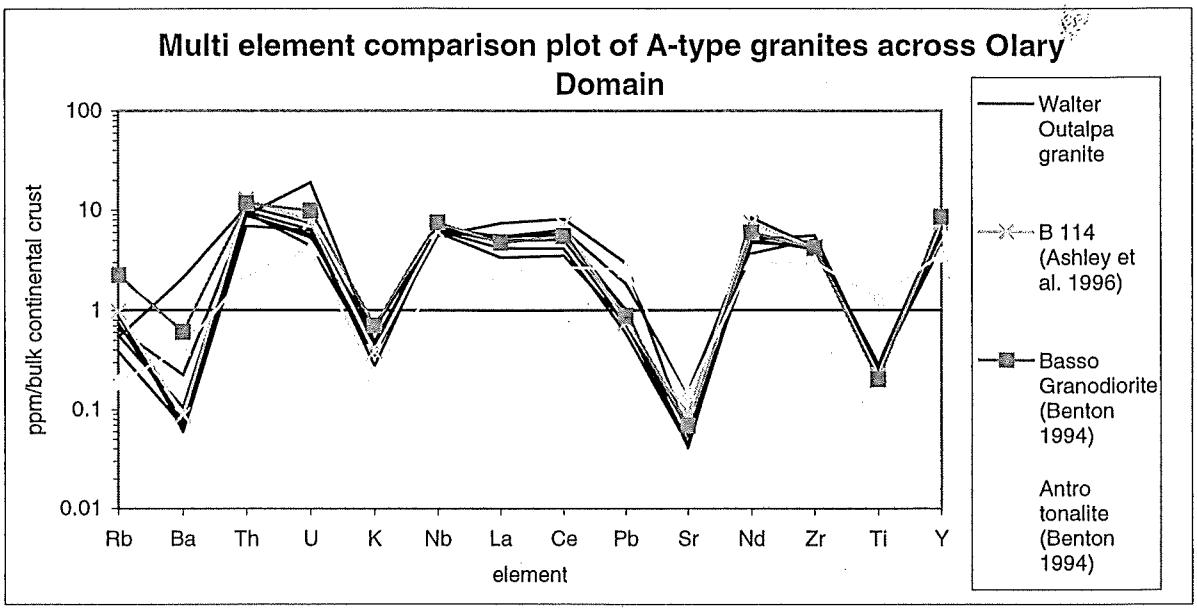

Figure 5.8

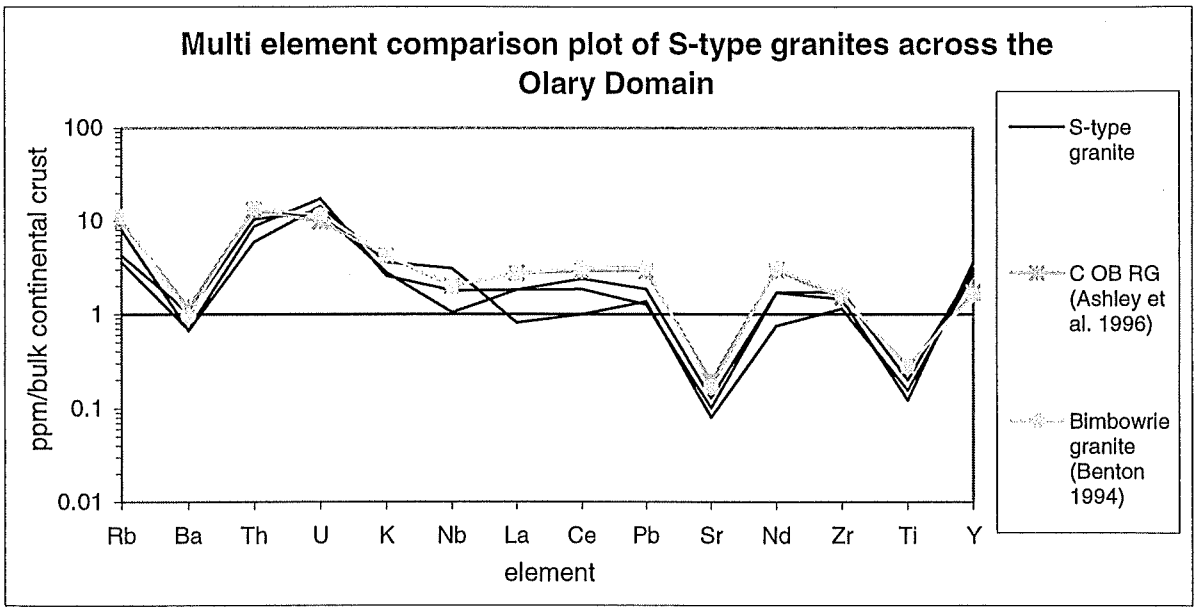

Figure 5.9

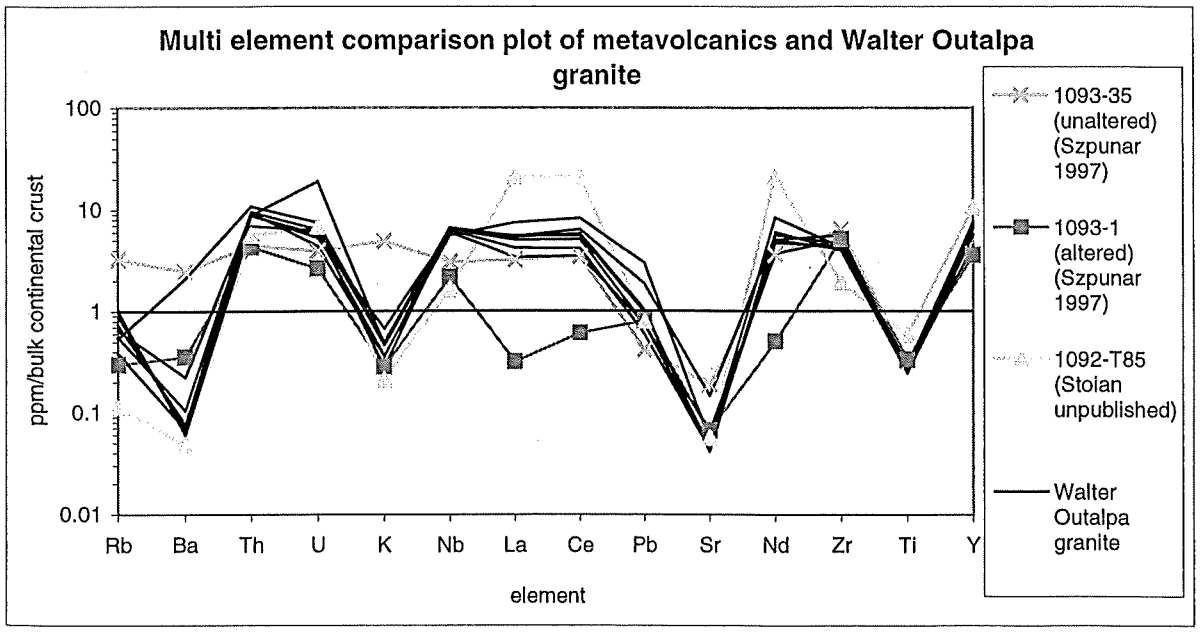

Painter Inlier (Neumann 1996). Using multi element plots (Fig 5.10 and 5.11), comparisons between the A-type granitoids of each province are illustrated. A problem arises when comparing granitoids of similar character as to whether the similarities relate to a unique source or whether the signal relates to magmatic processes.

There is no correlation between the Walter Outalpa granite and the Gawler Craton A-type intrusives. The Hiltaba Suite (1600-1585 Ma) is similar but these similarities probably relate to magmatic processes. Some similarities also exist between the Walter Outalpa granite and the Mount Neill granite and the Hot Springs Granitic Gneiss from Mount Painter. However, these Mount Painter intrusives are enriched in K, Th, and U. Again the Hot Springs granitic gneiss and Mount Neill granite are much younger (1575 Ma) than the Walter Outalpa granite and no correlation can be made.

Similarities in enriched A-type granitoids in South Australia, despite different ages in different provinces, suggests the A-type character is due more to magmatic processes rather than source composition.

5.4 Summary

- The Walter Outalpa granite, eastern and western Walter Outalpa granite sheets have very similar geochemical signatures while the peraluminous granite differs from this group.
- The far western granite sheet (Fig 3.1) differs chemically from the Walter Outalpa granites.
- The Walter Outalpa granites have an A-type and WPG character.
- The peraluminous granite has a geochemical signature typical of a crustal source. It has a WPG S-type character.
- During emplacement of the mafic enclaves trace element diffusion occurred between it and the Walter Outalpa granite giving the enclaves unique geochemical signatures and similarities to the host.
- The Walter Outalpa granites are chemically similar to other A-type granites within the Olary Domain.
- The peraluminous granites are chemically similar to other granites in the Olary Domain previously interpreted as S-type.

Figure 5.10

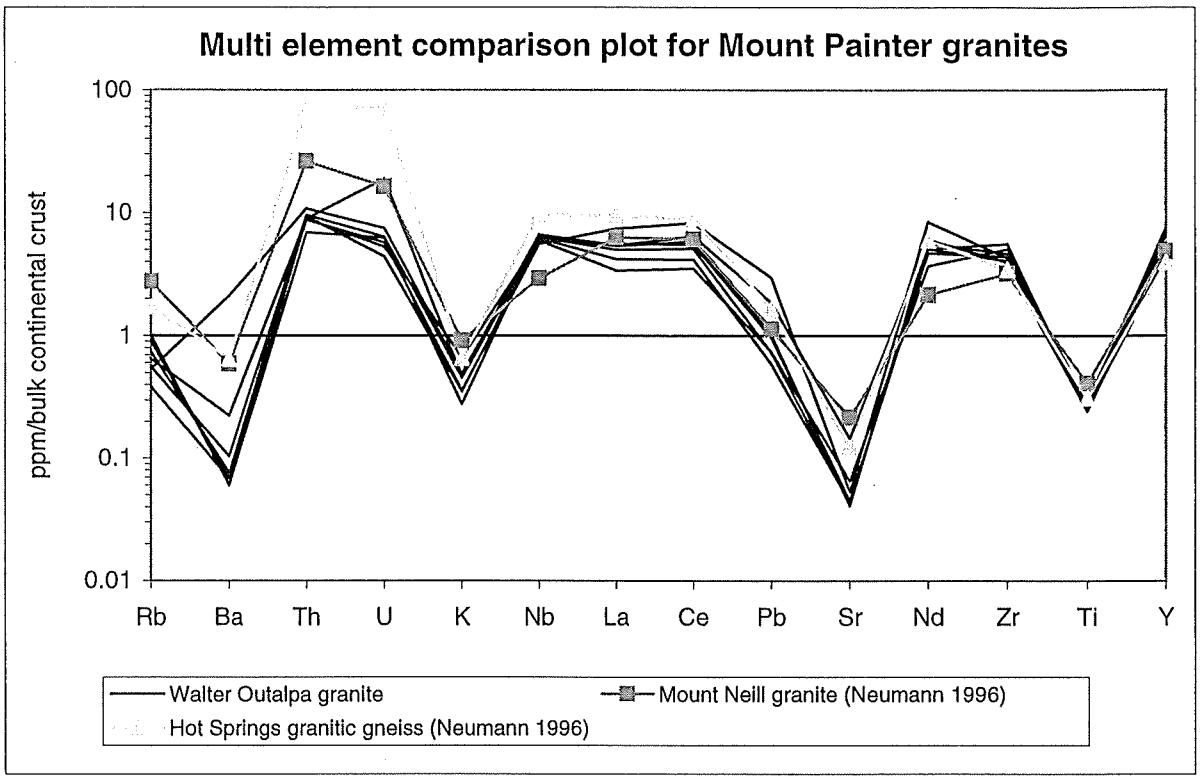

Figure 5.11

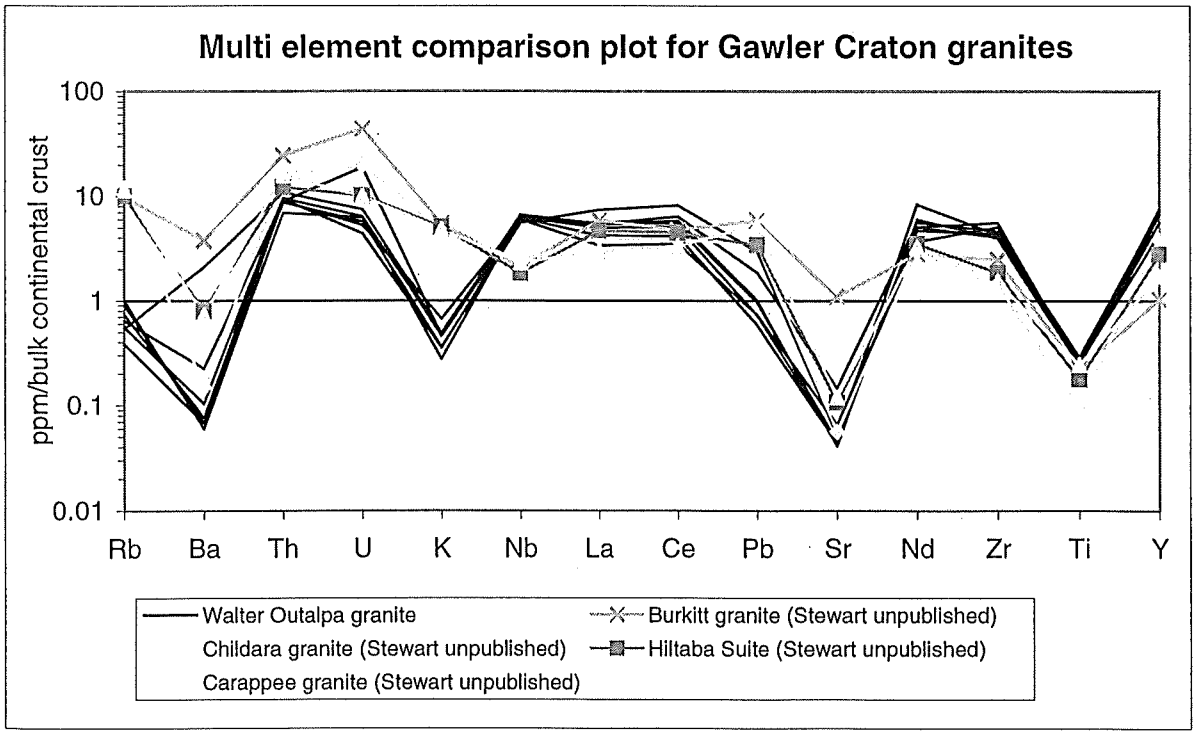

CHAPTER SIX:
ISOTOPE GEOLOGY

An isotopic study of the intrusives has been included to aid in the correlation between the mapped granitoids. This data set is also used to identifying both geological processes, age of mantle extraction and sources region.

6.1 Isotopic results

Samples selected for Sm-Nd and Rb-Sr isotope analysis include three granites bodies related to the Walter Outalpa granite, a mafic enclave, two peraluminous granite samples (one from within the map area and one from the central Weekeroo Inlier) and the amphibolite. The results are tabulated in Table 6.1.

Little reliance has been given to the Sr isotope results because the scattered results and several $^{87}Sr/^{86}Sr$ (T) values are unrealistically low. The high Rb/Sr ratios responsible for these unreliable and unusable results may relate to a post-emplacement alteration event where Rb and/or Sr have been mobile.

The Sm-Nd is a more robust isotope system and hence show greater consistency except for the mafic enclave sample (Sm/Nd = 0.42). Initial epsilon Nd ratios for the Walter Outalpa granites range from -0.67 to -1.22 while the peraluminous granite has values -2.44 and -3.84. Depleted mantle model ages for the Walter Outalpa granites, range from 2.14 to 2.44 Ga while those for the peraluminous granite ranges from 2.48 to 2.68 Ga. From the geochemical data (chapter five) it was suggested that the Walter Outalpa granite is substantially different from the peraluminous granite. This is further demonstrated by the Nd isotope results.

The initial epsilon Nd ratio and model ages for the Walter Outalpa granites are consistent with those previously obtained for other Olary Domain A-types (Fig 6.1). There is, however, variation in the initial epsilon Nd ratio between the peraluminous granite and the Bimbowrie unit of Benton (1994) (Fig 6.2). This may be a result of variation in metasedimentary source rocks in the two inliers.

Table 6.1 Summary of isotopic data.

sample no.	1106-003	1106-012	1106-032	1106-033	1106-036	1106-048	1106-053
rock	Peraluminous granite	Mafic Enclave	Amphibolite	Peraluminous granite	Western Walter Outalpa granite sheet	Eastern Walter Outalpa granite sheet	Walter Outalpa Granite
Nd ppm	30.03	11.00	14.78	25.52	*40.00*	82.18	72.67
Sm ppm	7.39	4.70	3.95	6.36	8.05	20.06	18.36
143/144 Nd	0.512013	0.512498	0.512514	0.511962	0.511765	0.512027	0.512099
2 sigma	0.000007	0.000010	0.000008	0.000008	0.000011	0.000009	0.000007
Sm/Nd	0.2460	0.4273	0.2672	0.2493	0.2012	0.2440	0.2527
147Sm/144Nd	0.1488	0.2585	0.1616	0.1508	0.1217	0.1476	0.1529
143/144Nd ch	0.512638	0.512638	0.512638	0.512638	0.512638	0.512638	0.512638
143/144Nd dep	0.513108	0.513108	0.513108	0.513108	0.513108	0.513108	0.513108
T mod:chur	1.98	-0.35	0.54	2.24	1.77	1.89	1.87
T mod:dep	2.48	-2.20	1.67	2.68	2.17	2.41	2.44
eps Nd (0)	-12.187040	-2.734405	-2.427346	-13.186713	-17.026654	-11.920498	-10.510458
age (T)	1.59	1.65	1	1.59	1.7	1.7	1.7
143/144(T)	0.510458	0.509694	0.511453	0.510386	0.510405	0.510376	0.510390
143/144ch T	0.510582	0.510504	0.511347	0.510582	0.510439	0.510439	0.510439
eps Nd chT	-2.44	-15.87	2.07	-3.84	-0.67	-1.22	-0.95
Sr87/86	0.958966	0.940494	0.750614	0.992337	0.996993	0.722785	0.776008
2 sigma	1.99E-05	2.97E-05	1.14E-05	2.54E-05	1.70E-05	1.77E-05	2.94E-05
Sr ppm	33.98295	20.2524	289.3627	27.48172	18.3102	16.20042	18.87202
Rb ppm	136.2327	164.8203	132.3087	114.0573	126.1555	2.15628	21.69165
Rb/Sr	4.0089	8.1383	0.4572	4.1503	6.8899	0.1331	1.1494
frac 87	1.240657	1.238451	1.215779	1.244641	1.245197	1.212457	1.218812
at wtSr	87.599733	87.600963	87.613871	87.597521	87.597213	87.615803	87.612117
87Rb/86Sr	11.883737	24.082429	1.328470	12.342226	20.498394	0.385661	3.347752
87Rb/86Sr	11.883737	24.082429	1.328470	12.342226	20.498394	0.385661	3.347752
87/86(T)	0.687603	0.369581	0.731615	0.710505	0.496141	0.713362	0.694210

value in italics is from XRF annalysis

Figure 6.1

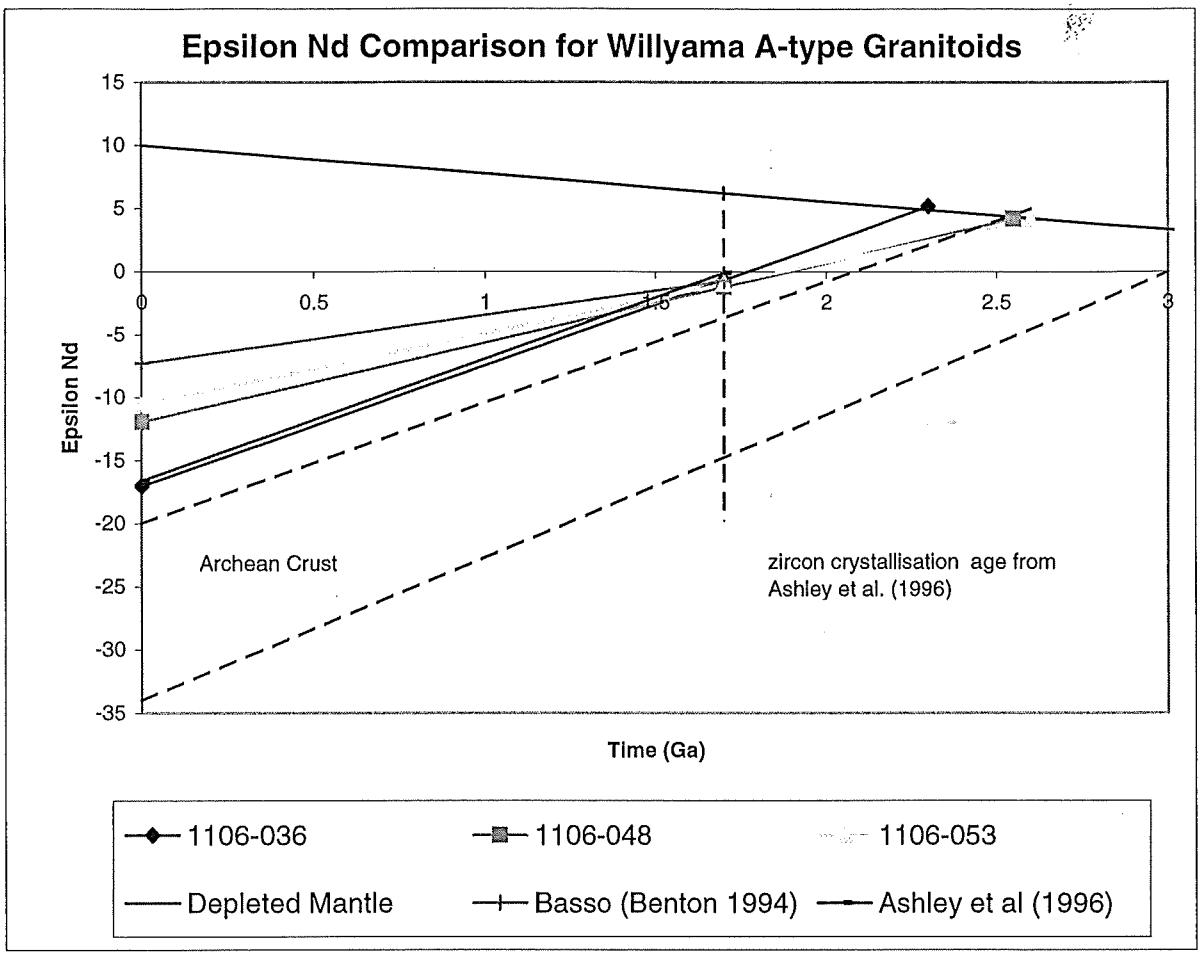

Figure 6.2

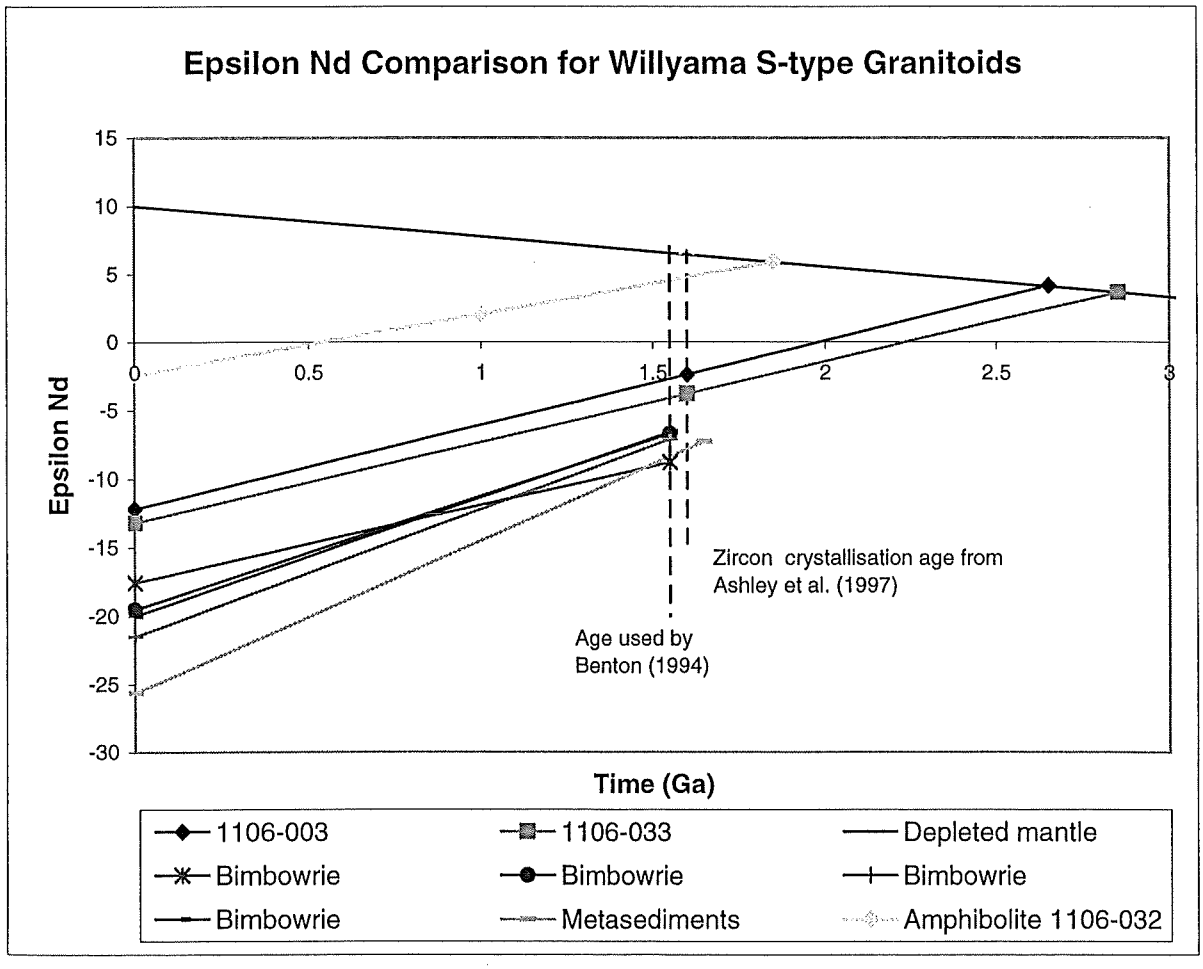

The unusual results for the mafic enclave make it hard to illustrate any link between this unit and its host, the Walter Outalpa granite. This result is perceived as being unusual because of unreasonably high Sm/Nd ratio which causes initial ratios to have a more evolved $^{144}Nd/^{143}Nd$ ratio. Partitioning of Sm by a mineral phase such as garnet could cause similar results. However, garnet is not present. The latest biotite partition coefficients for Sm and Nd also cannot explain this result (Charoy and Raimbault 1994). One possible reason for the distinct Sm/Nd ratio may relate to fractionation of the REE. The mafic enclaves display REE patterns which vary from LREE enriched to LREE depleted (Fig 5.5). The extremely low Sr isotope value may also be related to the process responsible for the high measured Sm/Nd ratio.

As previously mentioned, it is thought by many authors that the Olary Domain has been affected by a regional alteration event that has caused regional albitisation of the area. Such an event could reset isotopic systems and this should be taken into account when considering the isotopic data. Attempts at dating the albitisation have been inconclusive (Szpunar 1997).

6.2 Conclusion

Radiogenic isotope signatures within the Walter Outalpa granite are consistent, especially between the main Walter Outalpa granite and the eastern Walter Outalpa granite sheet. The western Walter Outalpa granite sheet differs marginally (as does its geochemistry). This suggests that the Walter Outalpa granites are part of the same intrusive and were one connected body when emplaced. The differing geochemical signature may relate to being less altered by the regional albitization due to its crystallisation position.

The consistent initial epsilon Nd ratio and depleted mantle model ages for the A-type granites in the Willyama Supergroup suggest that the geological processes responsible for these intrusives were regional. The isotopic data can be explained by two models for the generation of the A-type granites. These are illustrated below and in figure 6.3.

1. The Walter Outalpa granite (and other A-type granites across the Olary Domain) were separated from the mantle at their model ages (2.2 to 2.5 Ga) similar to the underplating model of Wyborn (1988). Here they evolved isotopically away from depleted mantle until a melting event of this protolith occurred at 1710 to 1700 Ma. Ascent followed, from lower crustal levels to the upper crust where it crystallised. The change in gradient at 1700 Ma relates to the higher partition coefficient for Nd compared to Sm. Such fractionation due to a melting event is not shown in figure 6.1 because the equation used

to determine the model ages of the granites maintains the same Sm/Nd ratio pre and post estimated crystallisation age.

2. The second model suggests depleted mantle and Archaean crust mixed in the lower crust at 1710 to 1700 Ma. Ascent from the lower to upper crust, followed with crystallisation occurring at shallow crustal levels at 1700 Ma (Fig 6.3). The relative proportions of lower crust and depleted mantle are speculative. However, figure 6.3 would suggest more Archaean crust than depleted mantle (say 60:40). This second, simpler model is preferred because only one melting event is required and a mechanism for melt generation is present.

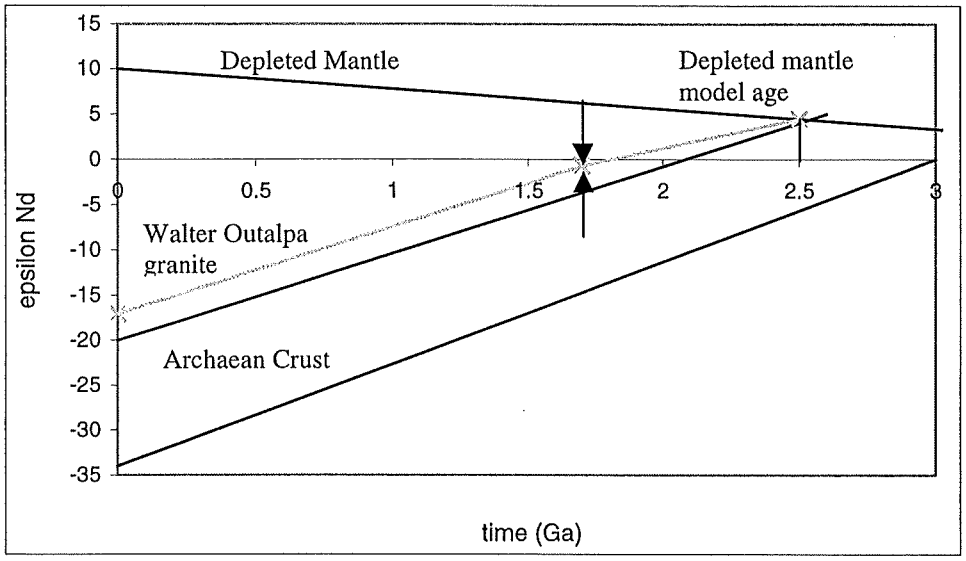

Figure 6.3 Epsilon Nd evolution models for the Walter Outalpa granite.

The peraluminous granite isotopic composition shows variation from its geochemical correlative, the Bimbowrie granite (Fig 6.2). This variation is source dependent. Theories to explain the regional difference in isotopes may include:

1. The peraluminous granite is a fractionated I-type granite with either a mantle or younger lower crust component.
2. The peraluminous granite assimilated younger rocks during ascent than the Bimbowrie granite.
3. The Bimbowrie granite has an older crustal source than the peraluminous granites.

The consistency between the Bimbowrie and metasediment isotopic results (Benton 1994) discounts explanation three. Similar isotopic studies across the Olary Domain regional granites are needed to constrain which model is correct. It would also reveal any geographical trend, which could be linked to tectonic models for the region, similar to those produced by Bennett and DePaolo (1987) for the western USA.

CHAPTER SEVEN:
EVOLUTION OF GRANITE GENERATION AND DEFORMATION FOR THE CENTRAL EASTERN WEEKEROO INLIER.

7.1 Magma generation and migration

Possible petrogenetic models for granitic melts include fractionation of the melt from the mantle, partial melting of crustal material, or some combination of these two processes. Based on isotopic and geochemical data it is possible to constrain the possible source region for the Walter Outalpa granite and the peraluminous granite outcropping in the central eastern Weekeroo Inlier. The isotopic data for the Walter Outalpa granites suggest possible sources to be Archaean or Palaeoproterozoic crust with a component of mantle mixing.

The problem then arises as to how melting of these sources occurred. A failed rift environment has been proposed for the deposition of the Willyama Supergroup (Willis et al. 1983). This is supported by conformable A-type volcaniclastic and granite units (Ashley et al. 1996). This study shows that the outcropping volcanic units from the eastern Weekeroo Inlier are chemically similar to the A-type Walter Outalpa granites.

Models for continental rifting predict partial melting of lower crust and mantle lithosphere due to mantle plume heating and/or basic magma intrusion and crystallisation (Creaser et al. 1991; Etheridge et al. 1987) (Fig 7.1A). It is believed that the Willyama Supergroup overlies Archaean crust, which would have been susceptible to partial melting and mixing with depleted mantle. This interpretation is supported by isotopic results (chapter six). The composition of this lower crustal source for A-type granites is speculative. Possibilities include tonalitic to granodioritic (Creaser et al. 1991) and charnockitic (Landenberger and Collins 1996). King et al. (1997) proposes a felsic infracrustal source, similar to that which could produce I-type granites, for the Lachlan Fold Belt A-type granites. The geochemical and isotopic consistency of the A-type granites across the Olary Domain suggests a single source.

Structural models for the deformation of the Walter Outalpa granite.

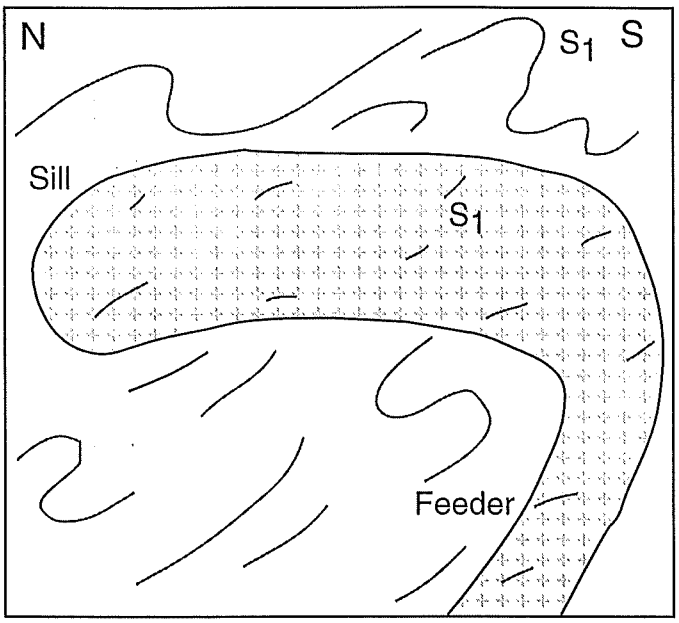

Figure 7.2

N-S schematic cross section.

Post emplacement deformation (D_1) developed the S_1 in the Walter Outalpa granite and metasediments. D_2 has folded S_1 and the feeder. This cross section is the current mapped surface and thus the Walter Outalpa granite displays a fold like geometry. The granite sheet now dips northeast.

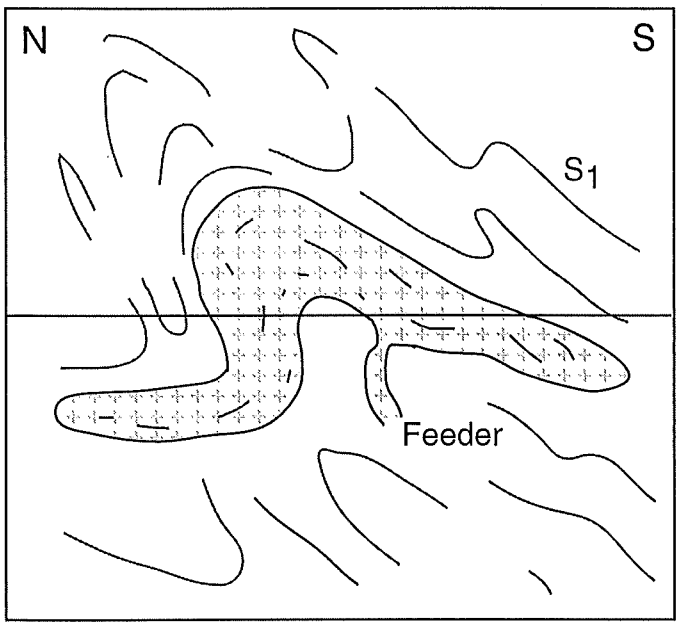

Figure 7.3

N-S schematic cross section.

During D_2 folding of both the metasediments and the Walter Outalpa granite occurred. This created a F_2 antiform in the granite with a northeast plunge.

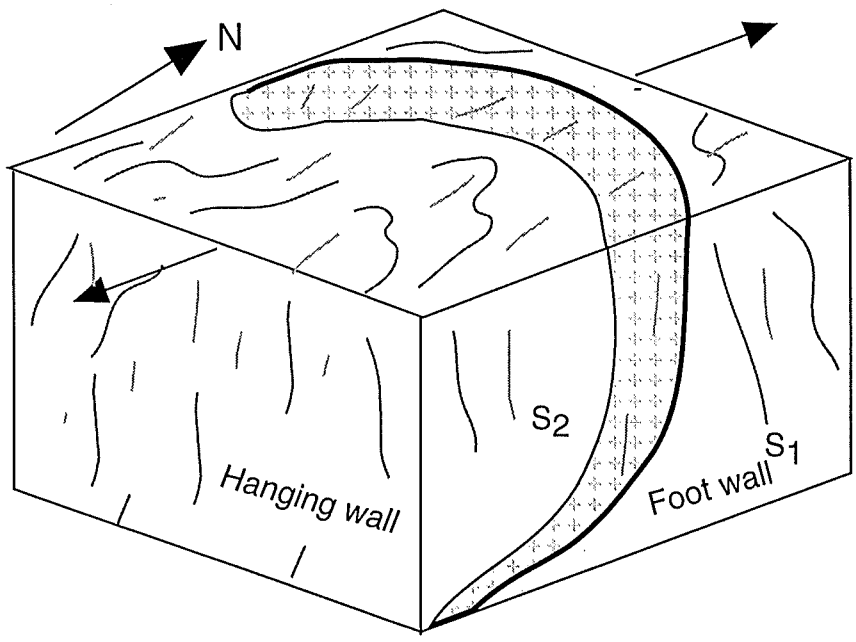

Figure 7.4

Schematic block diagram. Hutton (1988) proposesd emplacement of granitic magmas in listric faults developed along folded layering under extensional conditions where space is being created by relative movement between the hanging and foot walls. Emplacement of the Walter Outalpa granite in this model would be between D_1 and D_2 and thus the foliation in the intrusion is S_2.

A rifting environment also makes ascent of magma easier (Fig 7.1B). The Walter Outalpa granites display textures typical of a shallow level emplacement (graphic texture and absence of an aureole). Thus the Walter Outalpa granite has travelled far from its source. The preferred environment for dyke initiation is extensional but dykes may also form in contractional regimes (Weinberg 1996). Viscosity of A-type granites is typically low, because of the presence of fluorine, boron and high temperatures, facilitating large ascents and fast drainage of the source (Petford 1994). During ascent, fractionation of feldspar + quartz + biotite + hornblende + magnetite + zircon would result in a granite geochemically similar to the Walter Outalpa granites.

The emplacement of granite bodies requires space to be created, either by the process of intrusion through material transfer or a change in crustal thickness by, lowering of the Moho or displacing of the Earth's surface (Paterson and Fowler 1993). Various mechanisms to accommodate shallow level intrusives such as the Walter Outalpa granite include stoping, cauldron subsidence, wall rock translations (roof lifting) and sill/dyke fracturing (Paterson et al. 1991). Fracture opening in a regionally extensional environment due to felsic magma ascent is proposed and subsequent stoping and laccolith development is the preferred model for the emplacement of shallow granitoids (Paterson et al. 1991) such as the Walter Outalpa granite.

Intrusion into low temperature rocks ($<300^0$C) will cause steep thermal gradients. This gradient produces stresses of several kbars, providing a potential shattering mechanism and thus stoping (Paterson et al. 1991). It is this process which is favoured for the generation of the mafic enclaves. If this is correct then the fact that it is restricted to the northern contact suggests that younging at time of emplacement is now north. This is consistent with regional stratigraphy for the eastern Weekeroo Inlier (Clarke et al. 1986). Inverse metamorphic grading (Plate 2.a) is also consistent with this direction (Fig 4.1).

7.2 Regional deformation of the Walter Outalpa granite

The Olarian Orogeny is represented in the central part of the eastern Weekeroo Inlier by an S_1 layer parallel foliation, folding of this foliation by F_2 folds (F_3 folds of Berry et al. 1978) and retrograde shearing D_3. The structural evolution of the Walter Outalpa granite in relation to these deformations is discussed below where three possible timing relationships are illustrated.

Model one (Fig 7.2)
The development of a strong secondary tectonic foliation in the Walter Outalpa granite, overprints the primary graphic texture (Plate 2.d) and any preexisting magmatic foliation. This implies regional deformation began after complete crystallisation of the Walter Outalpa granites. Thus, the first model has intrusion of the Walter Outalpa granite pre D_1. D_1 then creates a layer parallel foliation in the metasediments and the tectonic foliation in the granite. D_2 follows folding S_1 in the metasediments and slight folding of the feeder sill geometry (Fig 7.2). This fold like geometry (Fig 3.1 and 4.1) appears to plunge to the northeast.

In this model emplacement is lateral in one direction (N) from the feeder (as opposed to the feeder being central as in model 2).

This model raises the question of why S_1 is not folded by F_2 folds in the Walter Outalpa granite. One explanation for this is a competency contrast across the wall rock intrusive contact. Supporting this contrast is the presence of shear zones at the contacts and transposition in the layered gneiss.

Model two (Fig 7.3)
This is similar to model one except, that here D_2 folds the granite into a regional scale F_2 fold with the major antiform (Fig 4.1) mapped in the layered gneiss representing a "Z" shaped fold. The western contact is locally overturned (Fig 4.2).

Model three (Fig 7.4)
Alternatively, the Walter Outalpa granite was emplaced between D_1 and D_2, to syn-tectonic with D_2. A similar model is proposed by Hutton, (1988) for the Strontian granite (a syn-tectonic granite). This interpretation would be consistent with Clarke et al's (1987) interpretation that the Walter Outalpa granite is syn-tectonic. This model requires listric fault contacts along strain heterogeneities. The reactivation of extensional listric faults associated with rifting as contractional listric faults during D_2 which extend beyond the Archaean crust into the Willyama Supergroup would have allowed rapid ascent of magma. This model also allows for stoping of wall rock or intrusion of mafic magma along the same listric fault to explain the mafic enclaves.

Model two is preferred because timing relationship imply a pre Olary Orogeny emplacement, absence of listric faulting and able to explain local overturning.

Figure 7.1 Tectonic model for the ascent and emplacement of the Walter Outalpa granite

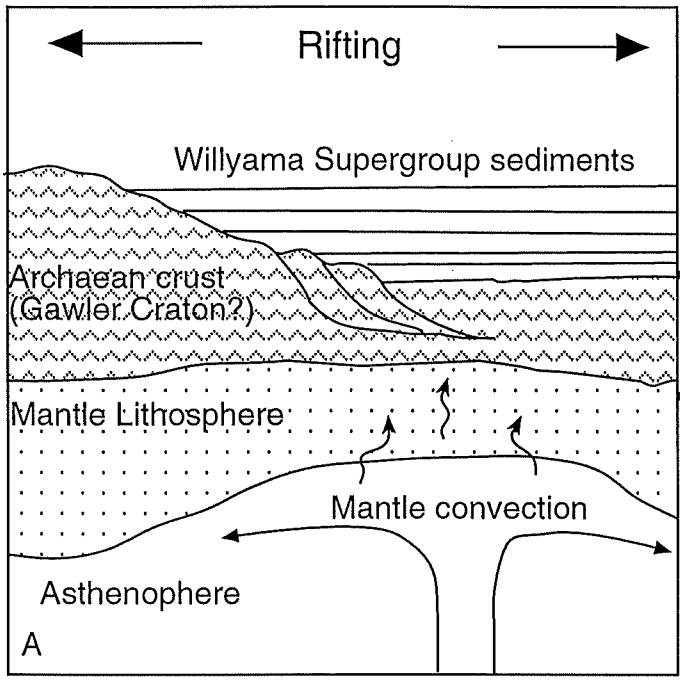

Continental rifting of Archaean crustal lithosphere initiated by the onset of small scale mantle convection. Basin formation allowed for the deposition of the Willyama Supergroup sediments. Rifting ceased prior to ocean crust formation.

Mantle upwelling is also responsible for the introduction of basic melt into lower crust.

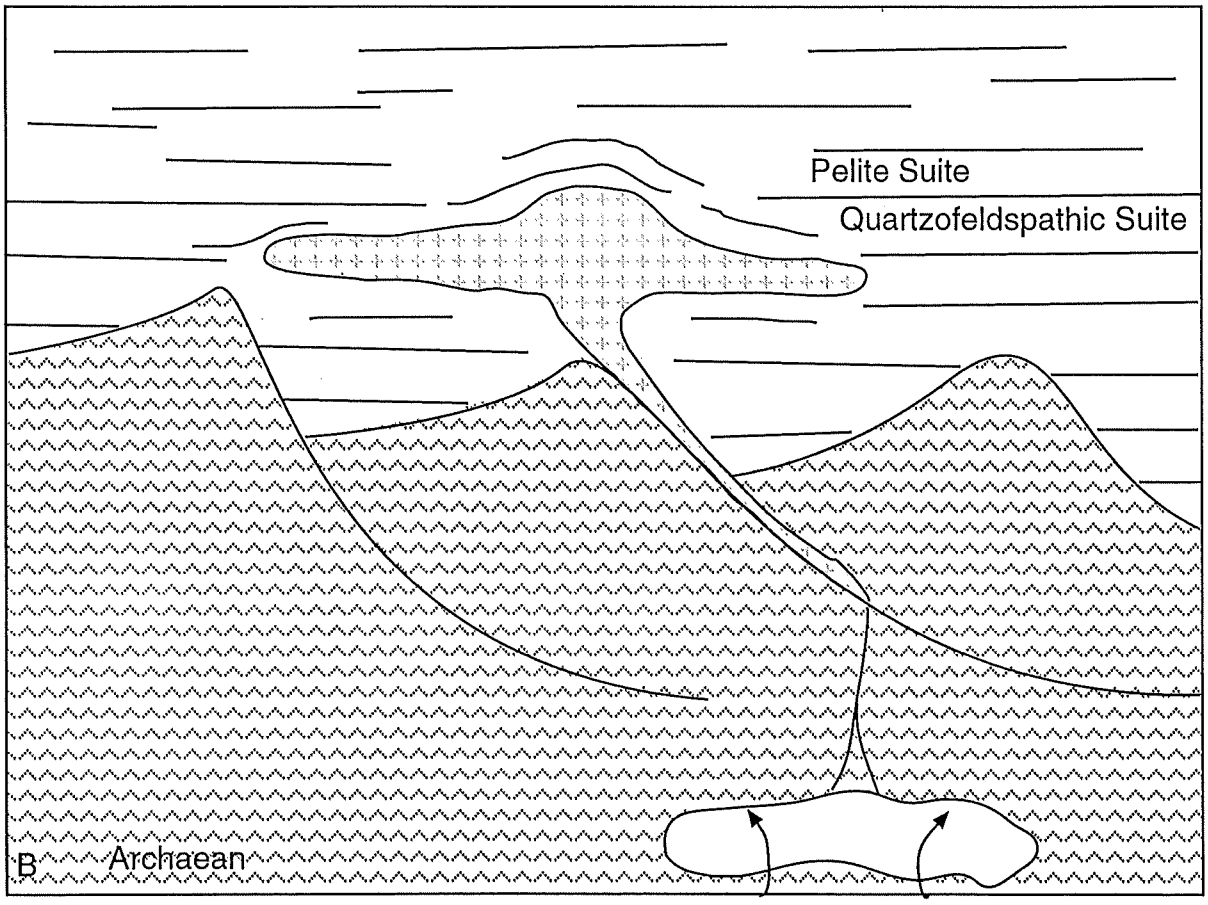

Partial melting of lower Archaean crust due to very elevated temperatures (900 - 950^{0}C) caused by mantle convection plus some input from the mantle. Ascent by dyking facilitated by extensional faulting. Sheet emplacement by horizontal fracture opening, stoping and laccolith development in the Willyama Supergroup.

7.3 Subsequent magma intrusions and deformations

The late tectonic nature of the peraluminous granite requires perturbed mid to upper crustal geotherms. Metamorphic conditions in the northern part of the eastern Weekeroo Inlier suggest amphibolite facies (Clarke et al. 1995). This, and the proposed thrust style of deformation (Clarke et al. 1986), implies minimal crustal thickening during the Olarian Orogeny. Thus generation of S-type granite was not by decompressional melting associated with modern orogenic belts having abnormal crustal thickening.

A model that could produce a hot crustal regime involves delamination of the mantle lithosphere due to mantle cooling and sediment load (Etheridge et al. 1987). This is proposed for the onset of the Barramundi Orogeny in northern Australia (Etheridge et al. 1987). Melting is caused by lower crust coming in contact with hot asthenosphere producing I-type granites during the Barramundi Orogeny (Etheridge et al. 1987). Similarities between this area and the Olary Domain include sediment deposition in a failed rift environment, thrust deformation and mixed Archaean crust depleted mantle magma generation. A similar lithospheric delamination process may have caused the onset of the Olary Orogeny.

A similar tectonic environment in the Olary Domain could produce the Olary Domain S-type granite geochemical signatures by high fractionation of a crust-mantle mixed source and assimilation of Willyama Supergroup metasediments. Alternatively, Olary Domain S-type granite may have formed by the intrusion, ascent and crystallisation of I-type granites at the Archaean crust Willyama Supergroup contact, causing melting of the Willyama metasediments. Density contrast across contacts can cause magma ascent to cease (Weinberg 1996).

In this second theory to explain the generation of the S-type granites, geotherms are perturbed to minimum melting temperatures for the Willyama Supergroup metasediments causing partial melting. This mode of magma generation produces near minimum melt composition magmas once critical melt fraction (van der Molen and Paterson 1979) is reached. Such melts would be slightly peraluminous (Chappell and White 1992). At such relatively low temperatures magma migration would be minor.

The latest Mesoproterozoic tectonic event to affect the central eastern Weekeroo Inlier was the retrograde shearing now depicted as the Walter Outalpa Shear Zone. This has displaced

the fold limb (or feeder or limb of the horseshoe geometry) horizontally by approximately three kilometres. It is also responsible for the tectonic fabric within the peraluminous granite, overprinting the tectonic foliation in the Walter Outalpa granite sheets and the presence of muscovite in the western Walter Outalpa granite sheet.

Following shearing, intrusion of the northeast southwest trending amphibolite dyke completed the geological evolution of the central eastern Weekeroo Inlier.

CHAPTER EIGHT:
CONCLUSION

Structural and petrologic study of previously undefined A-type and peraluminous Proterozoic intrusives in the eastern Weekeroo Inlier indicate that the intrusives are pre- and post-tectonic respectively. The area has been subject to three Olarian deformations. D_1 produced a layer parallel foliation, D_2 folded this foliation and D_3 relates to retrograde shearing. Of the various models proposed for the emplacement of the Walter Outalpa granite (chapter seven), model two is preferred. This model is preferred because it explains the presence of the overturned contact along the western contact of the Walter Outalpa granite and model three requires extension during compressional deformation.

Geochemistry and isotope geology can correlate and distinguish granitoid type in the Olary Domain. An example is the Walter Outalpa granite and granite sheets in the map area which show strong correlations although they have been variably affected by a post-emplacement alteration event. They are interpreted to be the same intrusive body. Geochemistry and isotope geology further distinguish the peraluminous granite as being a distinct unit and shows the granite sheet outside the map area is unrelated to the Walter Outalpa granite. These tools clearly differentiate between A- and S-type granites when used appropriately and give significant constraints on possible source regions and processes affecting the granites over their evolution. A regional study of the S-type granites would be beneficial to an understanding of their generation across the Olary Domain.

The presence of conformable comagmatic A-type volcanics and granites in the study area supports the previous interpretation of a rift or failed rift environment for the deposition of the Willyama Supergroup metasediments in the Olary Domain.

There are some similarities between the events leading up to and during the Olarian and Barramundi Orogenies. A mechanism similar to that invoked for the onset of the Barramundi Orogeny is proposed for the Olary Orogeny. Magmatic activity on the Gawler Craton of a similar age (Hiltaba Suite is 1580 Ma) may be related to the deformation recorded in the Olary Domain.

REFERENCES

Ashley, P.M., Cook, N.D.J. and Fanning, C.M., 1996. Geochemistry and age of metamorphosed felsic igneous rocks with A-type affinities in the Willyama Supergroup, Olary Block, South Australia, and implications for mineral exploration. *Lithos,* **38**: 167-184.

Ashley, P.M., Lawie, D.C., Conor, C.H.H. and Plimer, I.R., 1997. Geology of the Olary domain, Curnamona Province, S.A. *S. Australia Dep. Mines and Energy, Mineral Provinces South Australia Report Book* **97/17.**

Belperio, A.P., 1996. *Interpreted Solid Geology Lithostratigraphic Map, Olary Domain.* Department of Minerals and Energy, South Australia.

Bennett, V.C. and DePaolo, D.J., 1987. Proterozoic crustal history of the western United States as determined by neodymium isotopic mapping. *Geological Society of America, Bulletin*, **99**: 674-685.

Benton, R.Y, 1994. A petrographical, geochemical and isotopic investigation of granitoids from the Olary Province of South Australia – implications for Proterozoic crustal growth. *B.Sc Honours Thesis, University of Adelaide.*

Berry, R.F., Flint, R.B and Grady, A.E., 1978. Deformational history of the Outalpa area and its application to the Olary Province, South Australia. *Royal Society of South Australia Transactions,* **102**: 43-54.

Burnham, C.W. and Ohmoto, H., 1980. Late-stage processes of felsic magmatism. *Mining Geology, Special Issue* **8**: 1-11.

Chappell, B.W. and White, A.J.R., 1992. I- and S-type granites in the Lachlan Fold Belt. *Trans. Royal Soc. Edinburgh: Earth Sciences*, **83**: 1-26.

Chappell, B.W., White, A.J.R and Wyborn, D., 1987. The importance of residual source material (restite) in granite petrogenesis. *Journal of Petrology*, **28**: 1111-1138.

Charoy, B. and L. Raimbault L., 1994. Zr-, Th-, and REE-rich biotite differentiates in the A-type granite pluton of Suzhou (Eastern China): the key role of fluorine. *Journal of Petrology*, **35**: 919-962.

Clarke, G.L., Burg, J.P. and Wilson, C.J.L., 1986. Stratigraphic and structural constraints on the Proterozoic tectonic history of the Olary Block, South Australia. *Precambrian Research,* **34**: 107-137.

Clarke, G.L., Guirard, M., Powell, R. and Burg, J.P., 1987. Metamorphism in the Olary Block, South Australia: compression with cooling in a Proterozoic fold belt. *Journal of Metamorphic Geology* **5**: 291-306.

Clarke, G.L., Powell, R. and Vernon, R.H., 1995. Reaction relationships during retrograde metamorphism at Olary, South Australia. *Journal of Metamorphic Geology* **13**: 715-726.

Collins, W.J., 1998. Evaluation of petrogenetic models for Lachlan Fold Belt granitoids: implications for crustal architecture and tectonic models. *Australian Journal of Earth Sciences*, **45**: 483-500.

Cook, N.D.J. and Ashley, P.M., 1992. Meta-evaporite sequence, exhalative chemical sediments and associated rocks in the Proterozoic Willyama Supergroup, South Australia: implications for metallogenesis. *Precambrian Research,* **56**: 211-226.

Cook, N.D.J., Fanning, C.M. and Ashley, P.M., 1994. New geochronological results from the Willyama Supergroup, Olary Block, South Australia. *In*: Australian Research on Ore Genesis Symposium. *Adelaide, Australia Mineral Foundation,* **19**.1-19.5.

Cowely, W.M. and Flint, R.B., 1993. Epicratonic igneous rocks and sediments. *In* Drexel, J.F., Preiss, W.V. and Parker, A.J. (eds.) The geology of South Australia. Vol. 1, The Precambrian. *South Australia. Geological Survey. Bulletin,* **54**.

Cox, K.G., Bell, J.D. and Pankhurst, R.J., 1979. *The interpretation of igneous rocks.* George, Allen and Unwin, London.

Creaser, R.A., Price, R.C. and Wormald, R.J., (1991). A-type granites revisited: Assessment of a residual-source model. *Geology*, **19**: 163-166.

Etheridge, M.A. Rutland, R.W.R. and Wyborn, L.A.I., 1987. Orogenesis and tectonic process in the early to middle Proterozoic of northern Australia. *Proterozoic lithospheric evolution*, **17**. American Geophysical Union.

Fanning, C.M., 1995. Geochronological synthesis of southern Australia. Part 1 The Curnamona Province. *Prise.*

Flint, D.J. and Parker, A.J., 1993. Willyama Inliers. P.82-93. *In:* Drexel, J.F., Preiss, W.V. and Parker, A.J. (eds.) The geology of South Australia. Vol. 1, The Precambrian. *South Australia. Geological Survey. Bulletin,* **54**.

Forbes, B.G., 1991. Explanatory notes for the Olary 1:250 000 geological map. *Geological Survey of South Australia,* 47 p.

Freeman, H.S.R., 1995. A geochemical and isotopic study of mafic and intermediate rocks in the Olary Province, South Australia – magma series discrimination and geochronological framework. *B.Sc Honours Thesis, University of Adelaide.*

Glen, R.A., Laing, W.P., Parker, A.J. and Rutland, W.R., 1977. Tectonic relationships between the Proterozoic Gawler and Willyama orogenic domains, Australia. *Journal of the Geological Society of Australia*, **24**: 125-150.

Hobbs, B., Means, W. and Williams, P., 1976. *An Outline of Structural Geology.* Wiley.

Hutton, D.H.W., 1988. Granite emplacement mechanisms and tectonic controls: inference from deformation studies. *Trans. Royal Soc. Edinburgh: Earth Sciences*, **79**: 245-255.

King, P.L., White, A.J.R., Chappell, B.W. and Allen, C.M., 1997. Characterization and origin of aluminous A-type Granites from the Lachlan Fold Belt, southeastern Australia. *Journal of Petrology,* **38**: 371-391.

Laing, W.P., 1995. Interpreted solid geology lithostratigraphic map, Olary Domain, Curnamona Province 1:100 000 scale. *Geological Survey of South Australia.*

Laing, W.P., 1996. Nappe interpretation, palaeogeograph and metallogenic synthesis of the Broken Hill-Olary Block. *Codes Special Publication,* **1**: 21-51.

Landenberger B. and Collins W.J., 1996. Derivation of A-type granites from a dehydrated charnockitic lower crust: evidence from the Chaelundi Complex, eastern Australia. *Journal of Petrology*, **37**: 145-170.

Lottermoser, B.G. and Lu, J., 1994. Rare-element pegmatites in the Proterozoic Olary Block, South Australia. In: Australian Research on ore Genesis Symposium. *Adelaide, Australian Mineral Foundation*, 8.1-8.5.

Majoribanks, R.W., Rutland, R.W.R., Glen, R.A. and Laing, W.P., 1980. The structural and tectonic evolution of the Broken Hill region, Australia. *Precambrian Res.*, **13**: 209-240.

Mawson, D., 1912. Geological investigations in the Broken Hill area. *Royal Society of South Australia.* **11**: 211-319.

Neumann, N.L., 1996. Isotopic and geochemical characteristics of the British Empire Granite as indicators of magma provenance and processes of melt generation in the Mount Painter Inlier, South Australia. *B.Sc Honours Thesis, University of Adelaide.*

Paterson, S.R. and Fowler, T.K., 1993. Re-examining pluton emplacement processes. *Journal of Structural Geology*, **15**: 191-206.

Paterson, S.R., Vernon, R.H. and Fowler, T.K., 1991. Aureole tectonics. In: *Contact Metamorphism* (edited by Kerrick, D.M.). *Mineral Society of America. Reviews in Mineralogy*, **26**: 673-722.

Paterson, S.R., Vernon, R.H. and Tobisch, O.T., 1989. A review of criteria for the identification of magmatic and tectonic foliations in granitoids. *Journal of Structural Geology* **11**: 349-363.

Pearce, J.A., Harris, N.B.W. and Tindle, A.G., 1984. Trace element discrimination diagrams for the tectonic interpretation of granitic rocks. *Journal of Petrology*, **25**: 956-983.

Petford, N., Lister, J.R. and Kerr, R.C., 1994. The ascent of felsic magmas in dykes. *Lithos*, **32**: 161-168.

Ramsey, J.G. and Huber, M.I., 1987. *The techniques of modern structural geology, 2: Folds and Fractures.* Academic Press, London.

Rollinson, H., 1993. *Using geochemical data: evaluation, presentation, interpretation.* Longman Scientific and Technical, Essex.

Schofield, D.I. and D'Lemos, R.S., 1998. Relationships between syn-tectonic granite fabrics and regional PTtd paths: an example from the Gander-Avalon boundary of NE Newfoundland.. *Journal of Structural Geology* **20**: 459-471.

Stevens, B.P.J., Barnes, R.G. and Forbes, B.G., 1990. Willyama Block – regional geology and minor mineralization, *in* Hughes, F.E. (ed.) Geology of the mineral deposits of Australia and Papua New Guinea. *Australasian Institute of mining and Metallurgy, Monograph,* **14**: 1065-1972.

Szpunar, M.A., 1997. Structural and geochemical investigation of Proterozoic crustal evolution in the Weekeroo area, Olary Domain, South Australia. *B.Sc Honours Thesis, University of Adelaide.*

Talyor, S.R. and McLennan, S.M., 1985. *The continental crust: its composition and evolution.* Blackwell, Oxford.

Tilley, D.B., 1990. The geology of the central eastern part of the Weekeroo Inlier. Olary District, South Australia. *B.Sc Honours Thesis, Flinders University.*

Tribe, I.R. and D'Lemos, R.S., 1996. Significance of hiatus in decreasing-temperature fabric development fabric development within syntectonic quartz diorite complexes, Channel Islands, U.K. *Journal of the Geological Society, London* **153**, 127-138.

van der Molen, L. and Paterson, M.S. 1979. Experimental deformation of partially melted granite. *Contribution to Mineral Petrology* **70**: 299-318.

Vernon, R.H., 1986. Evaluation of the "quartz eye" hypothesis. *Eon. Geol.,* **81**: 1520-1527.

Watson, E.B., and Harrison, T.M., 1983. Zircon saturation revisited: temperature and composition effects in a variety of crustal magma types. *Earth and Planetary Science Letters*, **64**: 295-304.

Weinberg, R.F., 1996. Ascent mechanism of felsic magmas: news and views. *Trans. Royal Soc. Edinburgh: Earth Sciences*, **87**: 95-103.

Wiebe, R.A., 1996. Mafic-silicic layered intrusions: the role of basaltic injections on magmatic processes and the evolution of silicic magma chambers. *Trans. Royal Soc. Edinburgh: Earth Sciences*, **87**: 233-242.

Whalen, J.B., Currie, K.L. and Chappell, B.W., 1987. A-type granites: geochemical characteristics, discrimination and petrogenesis. *Contribution to Mineralogy and Petrology,* **95**: 407-419.

Willis, I.L., Brown, R.E., Stroud, W.J. and Stevens, B.P.J. 1983. The early Proterozoic Willyama Supergroup: stratigraphic subdivision and interpretation of high to low-grade metamorphic rocks in the Broken Hill Block, New South Wales. *Journal of the Geological Society of Australia,* **30**: 195-224.

Wingate, M.T.D., Campbell, I.H., Compston, W. and Gibson, G.M., 1998. Ion microprobe U-Pb ages for Neoproterozoic-basaltic magmatism in south-central Australia and implications for the break up of Rodina. *Precambrian Research* **87**: 135-159.

White, S.H., Rothery, E., Lips, A.L.W. and Barclay, T.J.R., 1995. Broken Hill area, Australia as a Proterozoic fold and thrust belt: implications for the Broken Hill base-metal deposits. *Transactions of the Institute of Mining and Metallurgy* **106**: B1-B17.

Wyborn, L.A.I., 1988. Petrology, geochemistry and origin of a major Australian 1880-1840 Ma felsic volcanio-plutonic suite: A model for intracontinental felsic magma generation. *Precambrian Research*, **40/41**: 37-60.

Wyborn, L.A.I., Wyborn, D., Warren, R.G. and Drummond, B.J., 1992. Proterozoic granite types in Australia: implications for lower crust composition, structure and evolution. *Trans. Royal Soc. Edinburgh: Earth Sciences,* **83**: 201-209.

ACKNOWLEDGEMENTS

The production of this thesis was aided by many people some of whom are acknowledged below. First of all I would like to thank my supervisors Pat James and Kathy Stewart for their advice, knowledge, enthusiasm, and putting up with my simple way of asking BASIC questions. They were great. Thanks to PIRSA for their financial support, use of their various resources and providing such an unsolvable problem. From PIRSA I would like to thank Colin Conor and Michael Szpunar for their input and local knowledge of the area.

A special mention must be made to my field partners – the Weekeroo Boys - Anthony Bottrill and Martin Beck and Betsy. Thanks for the good times in the field, especially the races. The Port Augusta Royal Flying Doctor Services also deserves my gratitude for making it possible to keep in contact with HQ, where the amazing Gerald Buttfield, Sondra Gould and Kim Crawford made sure I survived my tour of duty out at Weekeroo. Thanks to Thomas Flottmann for mapping advice and his camp oven cooking. Also deserving of acknowledgement are Will and Pauline Crawford for their hospitality at the Weekeroo Station and Glen Hunt for his special fish at the Mannahill Pub.

I also would like to thank Eike Paul, Naralle Neumann and the Structural Boys (Botts and Tiny plus Nic Nas) for discussions throughout the year. Their input was invaluable. Thanks also to the geophysics lads and Sandra McLaren for helping with the computing impossible.

Thanks must also go to the support stuff including Wayne Mussared, David Bruce, John Stanley and Sherry Proferes for their various skills, which made my project possible.

Last but not least is the Honours crew who I had to *put up with* this year! They are a great bunch of guys. I will not forget them and hope in the years to come we stay in contact. Thanks to Ned Ryan for always being prepared to drink hard.

"..... only at the end do you understand." Emperor Palpatine (A long time ago).

APPENDIX A

GEOCHEMICAL ANALYTICAL TECHNIQUES

XRF ANALYSIS

Sample Preparation

Samples were crushed to a gravel size in a jaw crusher before being milled in a Cr Ni mill.

Major element analysis

Powders were dried for two hours at 110^0C to remove any absorbed moisture. Weighed samples into crucibles were heated by an oven at 960^0C overnight to determine the Loss on Ignition (LOI) values. This includes organic matter and such gases as CO_2 and H_2O. In order to create fused discs one gram of sample is added to 4 grams of flux (Type 12:22 – 35.3% lithium tetraborate and 64.7% lithium metaborate). Fusion occurs at approximately 1150^0C under a propane-oxygen flame in Pt-Au crucibles.

Analysis was performed by a Philips PW 1480 X-ray Fluorescence Spectrometer using a dual anode (Sc-Mo) X-ray tube operating at 40kV, 75mA. Calibration was against several international and local Standard Reference Material (SRM's).

Results are presented as weight percent oxides, with both ferrous and ferric Fe expressed as Fe2O3T. These oxides include:
SiO2, Al2O3, FeO3T, MnO, CaO, Na2O, K2O, TiO2, P2O5, SO3.

Trace element analysis

About 5 grams of powdered sample was mixed with 1ml of binder solution (Poly Vinyl Alcohol) and pressed into a pellet. This was allowed to dry in air then heated to 60^0C in an oven for two hours to completely dry the sample prior to analysis.

Analysis was performed by a Philips PW 1480 X-ray Fluorescence Spectrometer incorporating several analysis programs covering suites of 1 to 7 trace elements, with conditions optimised for the elements being analysed. The programs were calibrated against many local and international SRM's. The dual-anode Sc-Mo tube (operated at sufficient voltage to excite the Mo) and an Au tube were used for the analyses. Matrix corrections are made using either the Compton Scatter peak, or mass absorption coefficients calculated from the major element data.

APPENDIX B

ISOTOPE ANALYTICAL TECHNIQUES

Isotope analysis

Approximately 200mg of milled sample was weighed out and added to a HF/HNO3 (hydrofluoric acid / nitric acid) solution used for digestion in a teflon vessel emplaced within a steel autoclave. Teflon bombs were used to decompose samples and ensure that all the refractory minerals such as zircon and monazite were completely dissolved. These vessels were then placed in an oven at 180^0C and over a period of 5 days additional HF was added for complete dissolution. Approximately 2 drops of a Sm-Nd (^{150}Nd-^{147}Nd) spike solution was added to 1/2 of the dissolved solution for determination of element concentrations.

Rubidium, strontium and the REE's were separated by standard cation exchange columns using HCl as an elutant. Neodymium and samarium were further separated using cation resin columns of teflon and HDEHP, again HCl as the elutant. Neodymium and samarium were loaded on tantalum side filaments opposing a rhenium filament. Strontium was loaded on single rhenium filaments prepared with phosphoric acid. Measurements were made on Finnigan Mat 261 and 262 solid source mass spectrometers.